Dear Editor,

Please find attached our response to the comments of the two anonymous reviewers. In response to the comments of anonymous reviewer 1, who found our manuscript too long and gave several good suggestions on how to make the text more concise, we have substantially shortened and the manuscript. In particular the detailed description of the prevailing meteorology associated with each of the clusters has been shifted to the supplement. Moreover, the number of figures has been reduced to 9 by shifting two figures to the supplement and combining two figures into one.

In response to the comments by anonymous reviewer 2 we rephrased several statements to make the text more clear and remove all ambiguity. We have also rephrased the abstract and conclusion to better present the key findings of this study and have included the uncertainty of the numbers in Table 2.

A detailed point by point response to their comments and a marked up version of the manuscript with the changes made in the text can be found bellow.

We thank you for considering our manuscript for publication in ACP.

Best Regards,

Baerbel Sinha

Reviewer comment:
This manuscript describes the measurements of particulate matter over two years at a site on the Indo Gangetic Plain in India, and the interpretation of those measurements using clusters of atmospheric back trajectories. The manuscript contains some important data quantifying the contributions of long range transport to the air quality exceedances observed in this important and understudied part of the world. These are my comments:
Authors' response:
We thank reviewer #1 for her/his helpful comments which have improved the clarity of the presentation further.

Reviewer comment:
Page 11412 line 28: The wording used in this sentence is repeated on page 11413 line 6. Please rephrase.
Authors' response: We have rephrased Page 11412 line 28
Modification in text:
"Statistical analysis of large datasets–has been a popular tool for identifying source regions of particulate matter..."

Reviewer comment:
Page 11415 to 11417– The description of the meteorology of the region is very long and hard to follow without an accompanying figure. Please consider shortening this section and replacing the text with a diagram in the supporting information that shows the seasonality of the prevailing winds and pressure gradients.
Authors' response: We understand that the text is difficult to follow without accompanying figures. We have, therefore, included a figure showing sea level pressure, surface winds and 700 hPa winds for each season in the Supplement. (Supplementary Fig. 1) using the NCEP Reanalysis Derived data provided by the NOAA Physical Science Division, Boulder, Colorado, USA, from their web site at http://www.esrl.noaa.gov/psd.
However, it should be noted, that this is the first paper from IISER Mohali Atmospheric Chemistry Facility which presents measurements from all seasons. Therefore, a detailed description of the meteorology of the site is warranted. Moreover, there are substantial discrepancies regarding the surface winds, mostly pertaining to the winds speed, between the model output and our measured wind speed. The measured wind speeds (Table 1) are much higher than the modelled wind speeds. In fact the measured wind speed and wind direction close to the surface is frequently better represented by the 700 hPa winds, than it is by the surface or 850 hPa winds of the model output. This problem is not unique to this particular model and meteorological dataset but also applies to e.g. Figure 6 in Lawrence and Lelieveld., (2010). We, therefore, consider a detailed description of the meteorology necessary and have revised the text such that it now refers to and discusses the new figure in Supplement 1.
Modification in text:
P11415 line 12 after "During winter season, weak northerlies or north-westerlies and a weak, low-level anti-cyclonic circulation prevails in the NW-IGP." We have inserted "The surface pressure map, the surface winds and 700 hPa winds of NCEP Reanalysis derived data provided by the NOAA Physical Science Division, Boulder, Colorado, USA are shown in supplementary Figure 1 panel a) to c)."
P11415 line 14 after "Wintertime fog occurs frequently and is favoured by subsidence of air masses over the IGP, low temperatures, high relative humidity and low wind speeds (5 ms^{-1})" we inserted "However, ground level wind speeds at our site are generally not as low as the surface wind speeds of the NCAR Reanalysis dataset would suggest. The seasonally averaged experimentally observed wind speed is 4.4 ms^{-1} and not < 2 ms^{-1}. This underestimation of the surface wind speeds in the NW-IGP is not unique to this particular model and meteorological dataset but also applies to e.g. Figure 6 in Lawrence and Lelieveld (2010)."
P11416 line 3 after "These loo-winds are extremely hot and dry" we inserted "and are not adequately resolved by the NCEP Reanalysis meteorological dataset (Supplementary Figure 1, panel d-f), which shows a very moderate average surface wind speed of 1.5-2.5 ms^{-1} over the NW-IGP that stands in stark contrast to the observed average wind speed of 5.6 ms^{-1}."

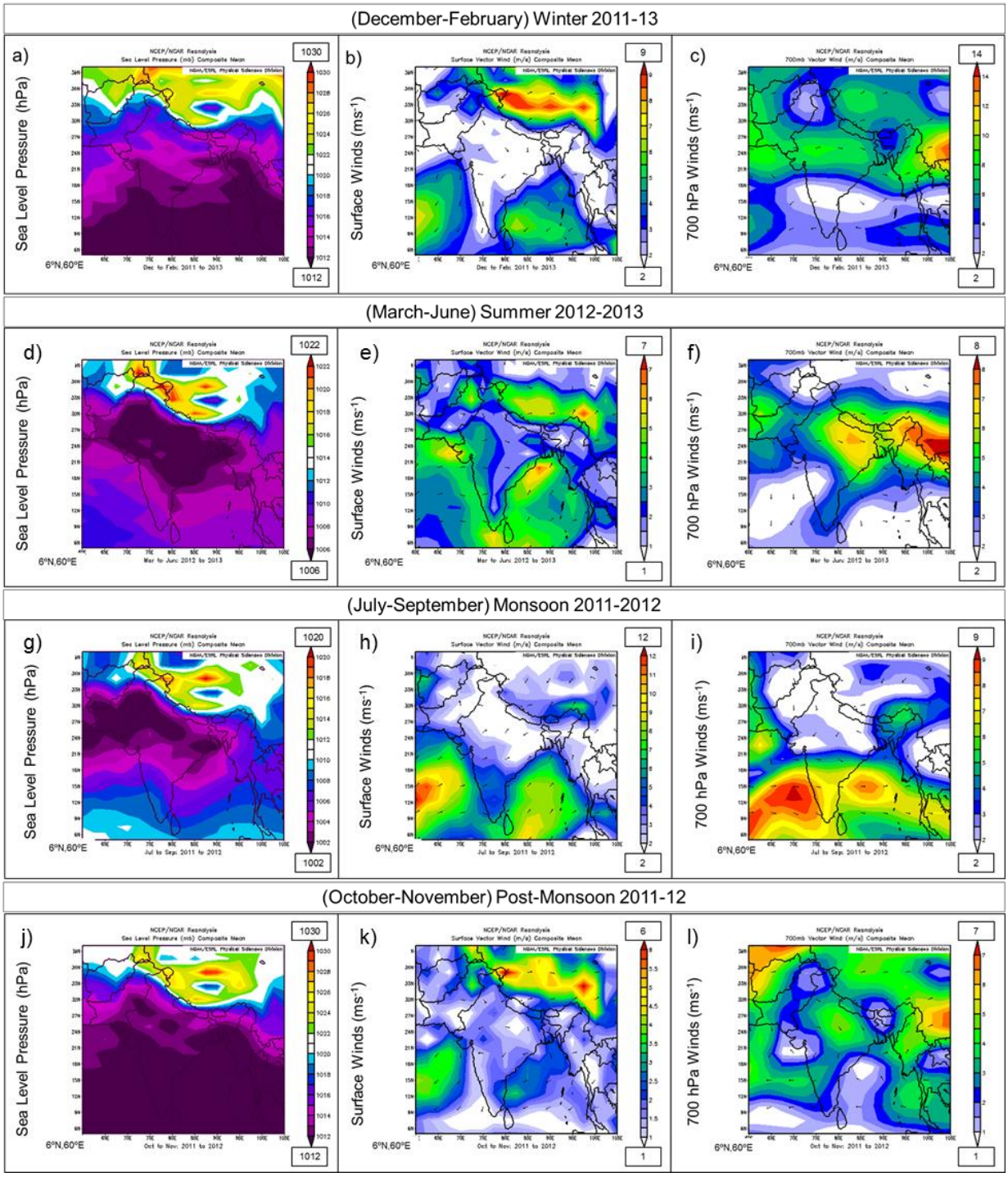

Supplementary Figure 1: Seasonal composites of sea level pressure, surface winds and 700hPa winds. The values on the top and bottom of the legend in each figure shows the maximum and minimum respectively. (Images provided by the NOAA-ESRL Physical Sciences Division, Boulder Colorado from their Web site at http://www.esrl.noaa.gov/psd/)

P11417 line 3 after "Break spells are associated with lower-tropospheric inversions, dusty winds and lower troposphere anti-cyclonic vorticity over the IGP (Sikka, 2003; Rao and Sikka, 2005; Bhat, 2006)." We inserted: "Both the observed wind direction and wind speeds of the surface winds during monsoon season are poorly resolved by the meteorological dataset. While the model suggests low wind speed (2 ms^{-1}) where south westerly winds dominate (Supplementary Figure 1, panel g-i), actual observations show that north westerly winds dominate during break spells and south easterly winds during active spells. The average wind speed is 5.1 ms^{-1}."

P1417 line 9 after "Winds are generally weak; the wind speed is less than 5ms^{-1} for more than 80% of the time." We inserted: "Post monsoon season shows the lowest discrepancy between modelled surface winds 1.5-2 ms^{-1} (Supplementary Figure 1, panel j-l) and observed average wind speeds 3.4 ms^{-1}. Surface wind vectors represent the observed night time flow at our site better, while the 700 ha Pa wind vectors represent daytime observations better. "

Reviewer comment: Figure 5 seems to provide an unnecessary level of detail.
Authors' response: While we agree that Figure 5 provides an extra dimension of detail, it is still relevant to the discussion. We have shifted Figure 5 to the Supplement. (Supplementary Figure 3)
Modifications in the text: Shifted Fig. 5 to the Supplement and modified the references to this figure in the text accordingly.

Reviewer comment: The paper is very long and details about the clusters might be best left to the supplemental.
Authors' response: We have shifted this information to the supplement.

Reviewer comment: There are too many figures in general. The number of figures should be less than 10.
Authors' response: We shifted Fig. 4 and Fig. 5 to the Supplement as Supplementary Figure 2 and Supplementary Figure 3 respectively. The information shown in figure 6 and figure 7 has now been shown on only one image and the text has been modified in accordance with this change. The total number of figures in the paper is now 9.

Reviewer comment: One suggestion is to add the average trajectory shown in Figure 6 onto the plot of all trajectories in Figure 7. The average trajectory could be shown by a black line amongst all the individual trajectories for each cluster.
Authors' response: We thank the reviewer for the suggestion. We have incorporated the average cluster trajectory onto the individual trajectories.

Reviewer comment: Figure 11: It is customary to include p values when presenting linear regression statistics. Also, the use of different colors in this figure is not explained. Also two regression equations are given. Why two? Figure caption needs more explanation.
Authors' response: We have only shown one regression line. The coefficient "a" represents the intercept and "b" represents the slope in the equation: $PM_{2.5} = a + b \times [Specie]$ where the specie maybe CO, NO_2, benzene or acetonitrile depending on the plot. With each plot, we have provided slope, error in slope and intercept and error in intercept.
We thank the reviewer for pointing it out that the information pertaining to what the coefficients "a" and "b" stand for in each of the linear regression plot was missing from the figure caption and we have included the same in the figure caption.
We did not mention p value rather we presented r^2 values as a goodness of fit parameter as is customary. Nevertheless, we did check the p value. It was less than 0.05 in each fit thus rendering the null hypothesis false.
We thank the reviewer for highlighting the missing colour index in the figure. The different colours represent different clusters.
Modifications in text: After incorporating the above discussed changes the figure caption is as follows:
"Figure 11: Scatter plots of fine mode PM with CO, NO2, acetonitrile and benzene and for winter, summer, monsoon and post-monsoon season. "a" stands for intercept , "b" stands for slope in the linear regression equation."

Reviewer comment: Figure 12: Caption includes the phrase: "during the daytime/nighttime low" which "low" is being referred to here?
Authors' comment: We thank the author for highlighting the missing information. The daytime and nighttime lows refer to the two minima observed in the diel-profile of coarse and fine mode PM. (Fig. 3); daytime: 12:00 to

16:00 LT and nighttime: 03:00 to 06:00 LT. We have now elaborated on the daytime/nighttime low in Figure 3 and its caption and lines 10-13, page 11417. The modifications have been shown below.

Modifications in text:

Modified Figure 3 and its caption

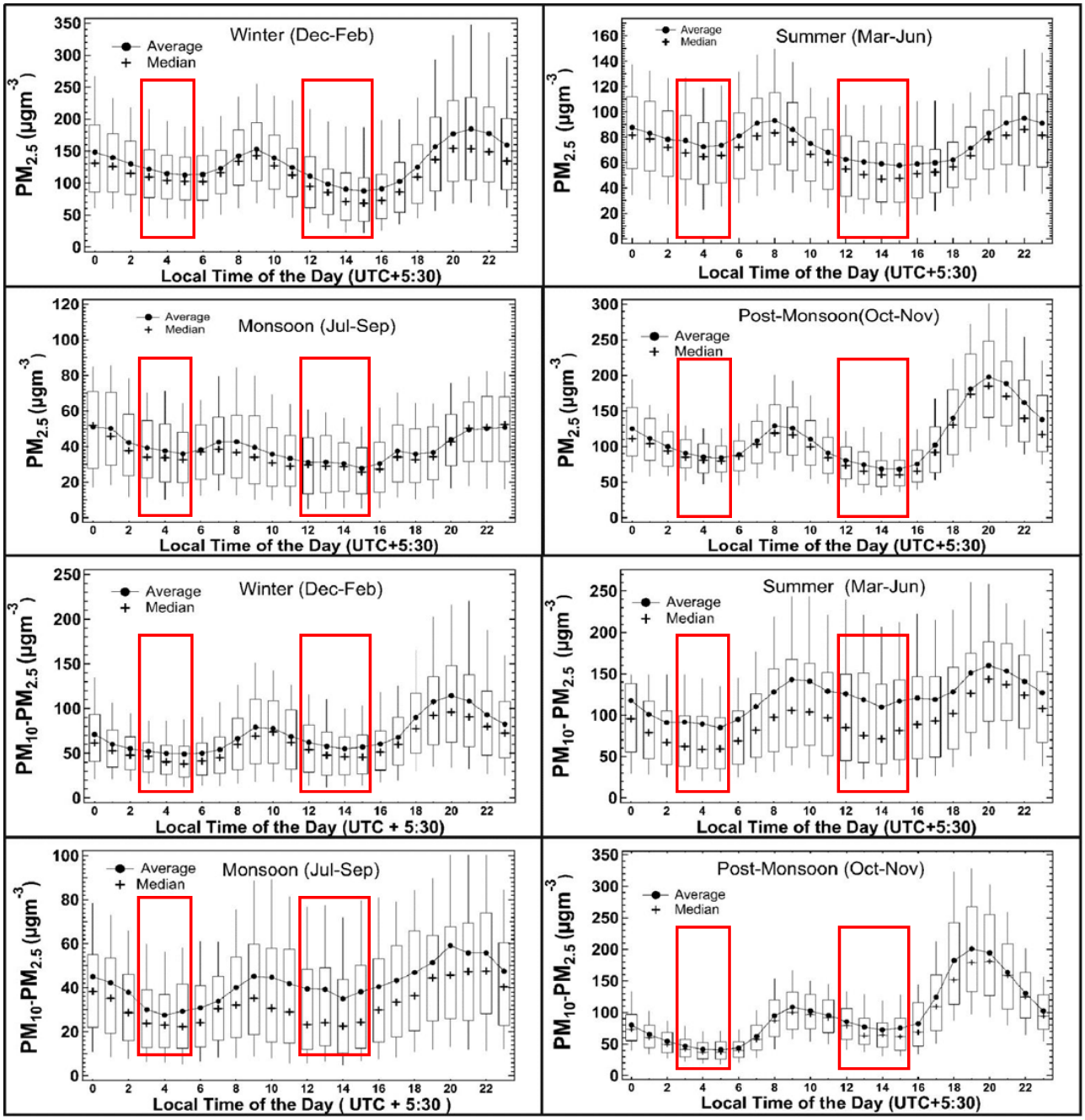

Figure 3: Diel box and whisker plots for fine mode (top four panels) and coarse mode (bottom four panels) particulate matter for winter, summer, monsoon and post monsoon season for the period November 2011 to August 2013 respectively. The box indicates the upper and lower quarter value; the cross indicates the median and the dots connected by lines provide the mean. The whiskers indicate the 5th and 95th percentile respectively. Periods of calm (WS <1ms^{-1}) have been excluded while preparing the graph. The interval highlighted in red shows the daytime low (12 to 4 p.m. LT) and nighttime low (3 to 6 a.m. LT).

Modified lines 10-13, page 11417
"Since the purpose of this study is to investigate the contribution of long range transport to PM pollution we restricted our analysis to measurements obtained between 12 noon to 4 p.m. LT (UTC+05:30) during the day and 3 to 6 a.m. LT (UTC+05:30) at night as depicted in Fig. 3 and consider calm conditions with wind speeds of less than 1ms^{-1} separately."

Reviewer comment: Also, it would be nice to know how many exceedance days there are in each season in addition to the percentages listed for each cluster.
Authors' comment: We thank the reviewer for asking this information as this prompted us to re-evaluate the number of exceedance days season-wise and while doing so we realized that using the average of the 4 hour time window of the minima instead of the 24 hour average while calculating the number of exceedance days is strictly speaking not correct. We have now used 24 hour averages and have included the information regarding the number of exceedance days in the text. We have also corrected the figure and the corresponding text. While the percentage of exceedance days may have changed, the main conclusion that the long range transport does not control % of exceedance days remains unchanged.
Modifications:
Modified Figure 12 and its caption with revised numbers and corrected the corresponding numbers in the text

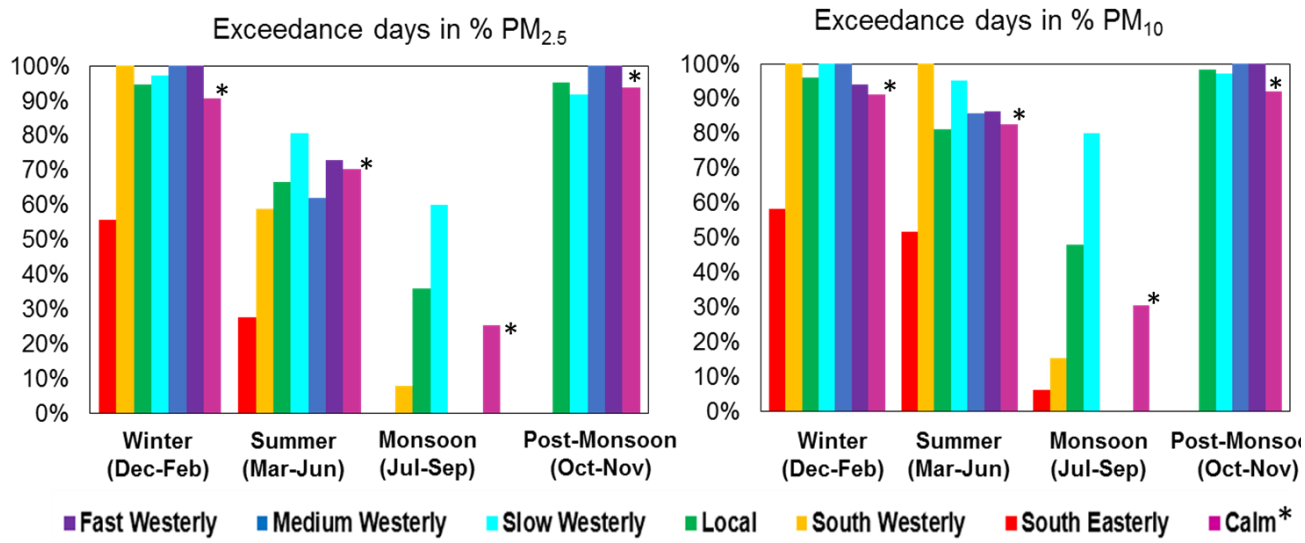

Figure 12. Percentage of days where the 24 hour average $PM_{2.5}$ or PM_{10} mass loading (in μgm^{-3}) exceeds the national ambient air quality standard for each air mass cluster and season.
* For calm conditions the $PM_{2.5}$ or PM_{10} were averaged for all times during a 24 hour interval that had WS < 1ms^{-1} only. The fraction of exceedance days is calculated based on this average, and not a genuine 24 hour average, as wind speeds do not remain low continuously.

Modified section 3.4 (page 11436-11439) to include % of exceedance days:

"3.4 Impact of air mass transport on Particulate Matter (PM) exceedance events
The mean PM mass loadings of an air mass cluster represent a poor proxy for the number of exceedance days that is the number of days on which 24 hour average PM_{10} or $PM_{2.5}$ exceeded the NAAQS of 100 μgm^{-3} or 60 μgm^{-3} respectively. During winter season on ~160 days (out of 180 days) NAAQS of both PM_{10} and $PM_{2.5}$ was exceeded. For summer season, exceedance days associated with PM_{10} were more frequent (203 out of 243 days) that those associated with $PM_{2.5}$ (157 out of 243). During monsoon season, the receptor site received cleaner air

masses with only 13 and 21 exceedance days (out of 92) of $PM_{2.5}$ and PM_{10} respectively. Post-monsoon season had frequent exceedance days with NAAQS of PM_{10} and $PM_{2.5}$ being exceeded ~ 110 out of 114 days.

While individual pollution episodes with extremely high PM mass loadings such as dust storms can profoundly influence the cluster mean, they barely affect the number of exceedance days as such events are rare. ”

References

Lawrence, M. G. and Lelieveld, J.: Atmospheric pollutant outflow from southern Asia: a review, Atmos. Chem. Phys., 10, 11017-11096, doi: 10.5194/acp-10-11017-2010, 2010.

Atmos. Chem. Phys. Discuss., 15, C4346–C4358, 2015
www.atmos-chem-phys-discuss.net/15/C4346/2015/

Atmospheric Chemistry and Physics Discussions

Interactive comment on "Quantifying the contribution of long-range transport to Particulate Matter (PM) mass loadings at a suburban site in the North-Western Indo Gangetic Plain (IGP)" *by* H. Pawar et al.

H. Pawar et al.

bsinha@iisermohali.ac.in

Received and published: 5 July 2015

[acpd, online, hvmath]copernicus

- **Reviewer comment:** This study aims to quantify the contribution of long range transport and local sources to PM loading at a station in IGP using back trajectory model and observational data at receptor site. In general, this paper is well written. The results are informative. The reviewer recommends to accept to publish

this study after some modifications and clarifications.

Authors' response: We thank reviewer #2 for this compliment and his/her helpful comments, which have improved the clarity of the presentation further.

- **Reviewer comment:**

  Major comments: Could you address the uncertainty and limitation of the quantifications derived from this study in order to guide the reader to apply the results later? -

  Authors' response: The uncertainties pertaining to figure 9 have already been presented in table 3, which provides the significance level for the difference of the mean for each pair of clusters. We have added the uncertainty of the enrichment above the regional background to table 2.

  Modifications in the text: The revised table(table 2) now reads as detailed below:

ACPD
15, C4346–C4358, 2015

Table 1. Lower limit for the contribution of long range transport and local pollution events to PM mass loadings in % $\pm$ 1σ of the total PM. "Negative" indicates that the PM mass loadings are not enhanced compared to the local cluster, which represent the regional background levels.

	Fast Westerly	Medium Westerly	Slow Westerly	South Westerly	South Easterly	Calm
			$PM_{2.5}$			
Winter	Negative	7 ± 4	13 ± 9	Negative	Negative	22 ± 15
Summer	20 ± 15	4 ± 3	31 ± 21	10 ± 8	Negative	13 ± 8
Monsoon	Negative	Negative	15	Negative	Negative	Negative
Post-Monsoon	18 ± 10	11 ± 7	Negative	Negative	Negative	Negative
			$PM_{10-2.5}$			
Winter	18 ± 8	28 ± 16	22 ± 15	9 ± 5	Negative	14 ± 10
Summer	57 ± 49	27 ± 21	34 ± 28	34 ± 26	Negative	Negative
Monsoon	Negative	Negative	29 ± 11	Negative	Negative	Negative
Post-Monsoon	27 ± 18	31 ± 21	9 ± 6	Negative	Negative	Negative

ACPD
15, C4346–C4358, 2015

- **Reviewer comment:** rewrite the abstract and conclusion parts. The currents ones are long and poorly organized, so it is hard for readers to capture the major signal. To synthesize and refine the results are needed.

  Authors' response and modifications in the text: We have shortened and restructured the abstract. The revised abstract now reads:

  ABSTRACT

  "Many sites in the densely populated Indo Gangetic Plain (IGP) frequently exceed the national ambient air quality standard (NAAQS) of 100 µg m^{-3} for 24 h average PM_{10} and 60 µg m^{-3} for 24 h average $PM_{2.5}$ mass loadings, exposing residents to hazardous levels of PM throughout the year.

  We quantify the contribution of long range transport to elevated PM levels and the number of exceedance events through a back trajectory climatology analysis of air masses arriving at the IISER Mohali Atmospheric Chemistry facility (30.667 N, 76.729 E; 310 m a.m.s.l.) for the period August 2011–June 2013. Air masses arriving at the receptor site were classified into 6 clusters, which represent synoptic scale air mass transport patterns.

  Long range transport from the west leads to significant enhancements in the average fine and coarse mode PM mass loadings during all seasons. The contribution of long range transport from the west and south west (Source region: Arabia, Thar desert, Middle East and Afghanistan) to coarse mode PM varied between 9 and 57 % of the total $PM_{10-2.5}$ mass.

  Local pollution episodes (wind speed < 1 m s^{-1}) contributed to enhanced $PM_{2.5}$ mass loadings both during winter and summer season and to enhanced coarse mode PM only during winter season.

  South easterly air masses (Source region: Eastern IGP) were associated with significantly lower fine and coarse mode PM mass loadings during all seasons.

ACPD
15, C4346–C4358, 2015

The fraction of days in each season during which the PM mass loadings exceeded the NAAQS was controlled by long range transport to a much lesser degree.

For the local cluster, which represents regional air masses (Source region: NW-IGP), the fraction of days during which the NAAQS of 60 µg m^{-3} for 24 h average $PM_{2.5}$ was exceeded, varied between 22 % and 85 % of the days associated with this synoptic scale transport during monsoon and winter season respectively ; the fraction of days during which the NAAQS of 100 µg m^{-3} for the 24 h average PM_{10} was exceeded, varied between 37 % during monsoon season and 84 % during winter season.

Long range transport was responsible for both, bringing air masses with a significantly lower fraction of exceedance days from the Eastern IGP and air masses with a moderate increase in the fraction of exceedance days from the West (Source region: Arabia, Thar desert, Middle East and Afghanistan).

In order to bring PM mass loadings in compliance with the NAAQS and reduce the number of exceedance days, mitigation of regional combustion sources in the NW-IGP needs to be given highest priority."

We have shortened and restructured the conclusion, the revised conclusion now reads:

CONCLUSION

We investigated the contribution of long range transport and local pollution episodes to the average coarse and fine mode PM mass loadings at our receptor site using two years of high temporal resolution data.The study yielded several results as follows:

1. Long range transport from the west Source region: Arabia, Thar desert, Middle East and Afghanistan)leads to significant enhancements in the average coarse

ACPD
15, C4346–C4358, 2015

mode PM mass loadings during all seasons. The contribution of long range transport from this source region to coarse mode PM varied between 9 % to 57 % of the totals $PM_{10-2.5}$ mass.

2. For fine mode PM the situation is more complex. The fast westerly cluster is associated with a 20 %increase in fine mode PM during summer and post monsoon season but cleaner air masses during winter season. The medium westerly cluster shows moderately enhance PM mass loadings during all seasons while slow westerly transport leads to enhanced $PM_{2.5}$ mass loadings during winter, summer and monsoon season but not during post monsoon season.

3. Local pollution episodes (wind speed $< 1\,m\,s^{-1}$)contributed to enhanced $PM_{2.5}$ mass loadings during both winter and summer season and to enhanced coarse mode PM only during winter season.

4. The south easterly cluster(Source region: Eastern IGP) is associated with significantly lower fine and coarse mode PM mass loadings during all seasons.

5. The number of days during which PM mass loadings exceed the national ambient air quality standard (NAAQS) of 100 $\mu g\,m^{-3}$ for 24 h average PM_{10} and 60 $\mu g\,m^{-3}$ for 24 h average $PM_{2.5}$ (NAAQS, 2009), however is controlled by long range transport to a much lesser degree.

   For the local cluster, which represents regional air masses (Source region: NW-IGP), the fraction of days during which the national ambient air quality standard (NAAQS) of 60 $\mu g\,m^{-3}$ for 24 h average $PM_{2.5}$ was exceeded varied between 22 % and 85 % of the days associated with this synoptic scale transport during monsoon season and winter season respectively; the fraction of days during which the national ambient air quality standard (NAAQS) of 100 $\mu g\,m^{-3}$ for the 24 h average PM_{10} was exceeded, varied between 37 % during monsoon season and 84 % during winter season.

ACPD
15, C4346–C4358, 2015

6. Long range transport was responsible for both bringing air masses with a significantly lower fraction of exceedance days from the Eastern IGP and air masses with a moderate increase in the fraction of exceedance days from the West (Source region: Arabia, Thar desert, Middle East and Afghanistan). The south easterly cluster (Source region: Eastern IGP) is always associated with a significantly lower fraction of exceedance days and the south westerly cluster also leads to a lower fraction of exceedance days during winter and monsoon season.

   Whenever long range transport increases the fraction of exceedance days the increase varies between a few percent and at most 30 %.

7. Fine mode PM ($PM_{2.5}$) contributes most to PM exceedance events at a regional level and $PM_{2.5}$ mass loadings are largely controlled by combustion sources during all seasons. Primary emission and gas to particle conversion of gas phase precursors emitted during the combustion, both contribute to the final mass loadings in varying proportions.

   In order to bring PM mass loadings in compliance with the national ambient air quality standard (NAAQS) and reduce the number of exceedance days, mitigation of regional combustion sources needs to be given highest priority as the number of exceedance days for air masses associated with the source region NW-IGP is already extremely high.

   To devise efficient mitigation strategies targeted at bringing down the number of PM exceedance events, a larger set of tracers needs to be incorporated and alternate source receptor modelling approaches e.g. PMF modelling targeted specifically towards identifying local and regional combustion sources contributing towards the emissions of PM and towards the emission gas phase aerosol precursors need to be adopted.

- **Reviewer comment:** Specific comments. - figure 2. A. What kind of wind do you plot here? Surface, 2m?

ACPD
15, C4346–C4358, 2015

Authors' response: We thank reviewer $\#2$ for pointing out that the height of the inlets and meteorological sensors was missing in our site description. It is 20 m above the ground level (a.g.l).

Modifications in the text: page 11414 after line 17 we inserted the following text. "The inlets of all instruments and the meteorological sensors are co-located and placed at a measurement height of 20 m a.g.l (Sinha et al., 2014)."

In the figure caption of figure 2 we inserted the following text. "Wind speed and wind direction were measured at a height of 20 m a.g.l."

- **Reviewer comment:** B. Have you checked the representativity of this station to NW IGP in terms of wind? In particular during monsoon season, the prevailing wind direction is south easterly instead of south westerly. Do you have any explanation?

  Authors' response: Yes, we have checked that the station is representative of the N.W. IGP for wind flow patterns. The Monsoon system is called the South-West Monsoon, but this name refers to its wind direction over the Indian Ocean and the southern peninsular. The monsoon cyclone enters the NW-IGP via the Bay of Bengal and the Eastern IGP (Bay of Bengal branch of the monsoon). Occasionally the low level jet enters through the Indus valley as the Arabian Sea branch of the monsoon circulation. The winds in the IGP run primarily parallel to the direction of the plains which are delineated by the Himalayan mountain range and the Aravelli Mountains. This applies to most of the IGP. It can be seen for e.g. in Goyal and Sidharth (2002) that even in New Delhi, at a site located more than 200 km South-Southeast from our site, and far away from the Himalayan mountain ranges W-NW and ESE-SE are still the two predominant wind directions during Monsoon season and south westerly winds are not very frequently observed.

- **Reviewer comment:** page 11418, line 21-22. What is GDAS dataset and which

ACPD
15, C4346–C4358, 2015

analysis database do you use? –

Authors' response: National Oceanic and Atmospheric Administration's **G**lobal **D**ata **A**cquisition **S**ystem (GDAS) is the meteorological data field used for the trajectory calculation, It originates from the GFS/GDAS (formerly FNL) archive and has been accessed via the Air Resource Laboratory (ARL) server. The full form of this abbreviation "National Oceanic and Atmospheric Administration's Global Data Acquisition System meteorology" has been mentioned on the same page line 11-13.

To make the text more clear, we have rephrased page 11418, line 11-13 and 21-22. Modifications in the text: page 11418, line 11-13 we have inserted the abbreviation (GDAS) after the full form and made the relevant first letters bold to facilitate the connection between the two "National Oceanic and Atmospheric Administration's **G**lobal **D**ata **A**cquisition **S**ystem (GDAS) meteorology."

page 11418, line 21 onwards we replaced "dataset" with "meteorological data field" throughout to improve the clarity of the text

- **Reviewer comment:** page 11419, line 4. Only 3 out of 27 are consistent with the measurement. Do you mean all seasons? How do you explain the low percentage and the representativity of the results from this study?

Authors' response:

The model terrain height for a given latitude longitude co-ordinate (place) in the input data (GDAS meteorological data field) of the NOAA hysplit model is independent of season. The actual true terrain height of the same place is well known. However, the meteorological data field used as model input has a 1 resolution and the terrain height for the latitude longitude pair entered as the starting coordinate for the trajectory run is interpolated from the closest grid points. This is done by the model itself and the interpolated terrain height does not always agree with the actual terrain height, in particular in the vicinity of mountain ranges. How

ACPD
15, C4346–C4358, 2015

many ensemble runs will give reasonable terrain heights both for our station in the plains and the mountain site Shimla, located 60 km to the NE of our site, depends on how the terrain is represented in the models input data field. While the modelled air mass origin is strongly affected by how well the mountain range is resolved in the model, we note that this sensitivity of the model does not affect the results of our study. We have selected only those 3 ensemble runs for which the GDAS meteorological data field provide appropriate terrain heights both for our site in the plains and for a mountain site located 60 km to the NE of our site. By doing this we have made sure that the model output we work with is unaffected. To make this clear we have inserted the text below page 11419 in line 7.

Modifications in the text: "To ensure that this sensitivity of the model does not affect the results of our study, we. . .."

- **Reviewer comment:** - page 11421, line 17. In the previous study, you mentioned that the optimum is 6, but you use seven cluster here. Why?

  Authors' response: We did not understand what the reviewer implies by "previous study". Page 11421, line 17 reads the "number of optimum clusters was 6."

- **Reviewer comment:** - page 11422, line 10. Did you mention figure 7 before figure 8?

  Authors' response: Yes, figure 7 is cited first on page 11421 in line 24 i.e. before figure 8.

- **Reviewer comment:** - page 11426, line 23. Should it be figure 9 instead of table3?

  Authors' response We thank reviewer $\#2$ for pointing out that reference in line 23 should be to figure 9. We corrected this and shifted the reference to table 3 to Page 11426 line 25.

ACPD
15, C4346–C4358, 2015

Modifications in the text: Shifted the reference.

- **Reviewer comment:** - page 11426, line 26 and page 11427, line 3. Could you specify what is the aqueous phase oxidation of gas phase precursors?

  Authors' response: Aqueous phase oxidation of gas phase precursors refers to a process wherein a gas (e.g. $NH_3(g)$, $SO_2(g)$, $NO_2(g)$) is taken up by aqueous phase aerosol and subsequently undergoes reactions that change the oxidation state resulting in the formation of ammonium, sulphate and nitrate ions. Upon drying, these precipitate out as salts which can be coarse in size.

- **Reviewer comment:** Can your study derive it? If not, list reference.

  Authors' response: In figure 10 we provide observational evidence that this process does contribute to coarse mode aerosol whenever the RH is high. We see a good correlation of CO and coarse mode PM at high RH but not at low RH. It is well known, that primary particulate emissions from combustion normally fall into the PM_1 size range and contribute little to PM with an aerodynamic diameter >2.5 μm. The fact that only when RH reaches levels that allow a significant aerosol aqueous phase to exist, a correlation of coarse mode PM with CO appears, indicates, that coarse mode salt formation via such oxidation reactions contributes to coarse mode PM. To make it more clear, that this statement refers to figure 10 we have restructured and modified the text.

  Modifications in the text: Figure 10 shows the correlation of CO with coarse mode PM ($PM_{10-2.5}$) as a function of meteorological conditions. It can be seen from this figure that two sources contribute prominently to coarse mode PM mass loading during winter: aqueous phase oxidation of gas phase precursors and dust. Aqueous phase oxidation of gas phase precursors refers to a process wherein gases (e.g. $NH_3(g)$, $SO_2(g)$, $NO_2(g)$) are taken up by aqueous phase aerosol and subsequently undergo reactions that change the oxidation state resulting in the formation of ammonium, sulphate and nitrate ions. Upon drying

ACPD
15, C4346–C4358, 2015

these precipitate out as salts which can be coarse mode in size.

- **Reviewer comment:** page 11436, line 11. Define the exceedance before section 3.4.1

  Modifications in the text: We have modified the first sentence of section 3.4 such that it now includes the definition:

  " The mean PM mass loadings of an air mass cluster represent a poor proxy for the number of exceedance events, that is the number of days on which the 24h average of $PM_{2.5}$ or PM_{10} exceeded the NAAQS of 60µg m^{-3} for 24h average $PM_{2.5}$ or 100µg m^{-3} for the 24h average PM_{10} respectively."

- **Reviewer comment:** – page 11437, line 4-6, page 11438, line 2-4, line 21-22, Give references.

  Authors' response: These statements are based on our own findings; we have revised these statements to make the source of these statements more clear.

  Modifications in the text:

  page 11437, line 4-6: " As discussed in section 3.3.2, during summer season,the ambient RH is usually < 60 % at night and 20-30 % during the day (Table 1) and aqueous phase oxidation contributes less to $PM_{2.5}$ and PM_{10} mass loadings."

  page 11438, line 2-4 we have shifted these lines to the end of the discussion and started the discussion with "Figure 12 shows that the . . ."

  page 11438, line 21-22: "As discussed in section 3.3.4, crop residue burning coupled with aqueous phase oxidation of gas phase precursors is responsible for high PM mass loading during post-monsoon season. It can be seen from figure 12 that it also contributes to a high frequency of exceedance events."

ACPD
15, C4346–C4358, 2015

References

Effect of winds on SO2 and SPM concentrations in Delhi, Atmospheric Environment, Volume 36, Issue 17, June 2002, Pages 2925-2930, ISSN 1352-2310, doi: 10.1016/S1352-2310(02)00218-2, 2002.

Sinha, V., Kumar, V., and Sarkar, C.: Chemical composition of pre-monsoon air in the Indo-Gangetic Plain measured using a new air quality facility and PTR-MS: high surface ozone and strong influence of biomass burning, Atmos. Chem. Phys., 14, 5921–5941, doi:10.5194/acp-14-5921-2014, 2014.

Manuscript prepared for Atmos. Chem. Phys. Discuss.
with version 2014/07/29 7.12 Copernicus papers of the LaTeX class copernicus.cls.
Date: 13 August 2015

Quantifying the contribution of long-range transport to Particulate Matter (PM) mass loadings at a suburban site in the North-Western Indo Gangetic Plain (IGP)

H. Pawar[1], S. Garg[1], V. Kumar[1], H. Sachan[1], R. Arya[1,2], C. Sarkar[1], B. P. Chandra[1], and B. Sinha[1]

[1]Department of Earth and Environmental Sciences, Indian Institute of Science Education and Research Mohali, Sector 81, S.A.S Nagar, Manauli PO, Punjab 140306, India
[2]School of Chemical and Biomolecular Engineering, Cornell University, Ithaca, New York, USA

Correspondence to: B. Sinha (bsinha@iisermohali.ac.in)

Abstract

Many sites in the densely populated Indo Gangetic Plain (IGP)frequently exceed the national ambient air quality standard (NAAQS) of 100 µg m^{-3} for 24 h average PM_{10} and 60 µg m^{-3} for 24 h average $PM_{2.5}$ mass loadings, exposing residents to hazardous levels of PM throughout the year.

We quantify the contribution of long range transport to elevated PM levels and the number of exceedance events through a back trajectory climatology analysis of air masses arriving at the IISER Mohali Atmospheric Chemistry facility (30.667° N, 76.729° E; 310 m a.m.s.l.) for the period August 2011–June 2013. Air masses arriving at the receptor site were classified into 6 clusters, which represent synoptic scale air mass transport patterns. BS: ~~and the average PM mass loadings and number of exceedance events associated with each air mass type were quantified for each season.~~

Long range transport from the west leads to significant enhancements in the average BS: fine and coarse mode PM mass loadings during all seasons. The contribution of long range transport from the west and south west (Source region: Arabia, Thar desert, Middle East and Afghanistan) to coarse mode PM varied between 9 and 57 % of the total $PM_{10-2.5}$ mass.

Local pollution episodes (wind speed < 1 m s^{-1}) contributed to BS: enhanced $PM_{2.5}$ mass loadings both during winter and summer season and to enhanced coarse mode PM only during winter season.

South easterly air masses (Source region: Eastern IGP) were associated with significantly lower BS: fine and coarse mode PM mass loadings during all seasons.

BS: ~~For fine mode PM too, transport from the west usually leads to increased mass loadings during all seasons. Local pollution episodes contributed to enhanced $PM_{2.5}$ mass loadings during winter and summer season. South easterly air masses were associated with significantly lower $PM_{2.5}$ mass loadings during all seasons. Using simultaneously measured gas phase tracers we demonstrate that most $PM_{2.5}$ originated from combustion sources.~~

The fraction of days in each season during which the PM mass loadings exceeded the national ambient air quality standard was controlled by long range transport to a much lesser degree.

For the local cluster, which represents regional air masses (Source region: NW-IGP), the fraction of days during which the national ambient air quality standard (NAAQS) of 60 µg m^{-3} for 24 h average $PM_{2.5}$ was exceeded, varied between BS: ~~22~~ BS: 36 % BS: and 95 % of the days associated with this synoptic scale transport during monsoon BS: and post monsoon and winter season BS: respectively BS: ~~and 85 % of the days associated with this synoptic scale transport during winter season~~; the fraction of days during which the BS: ~~national ambient air quality standard (NAAQS)~~ NAAQS of 100 µg m^{-3} for the 24 h average PM_{10} was exceeded, varied between BS: ~~37~~ BS: 48 % during monsoon BS: ~~season~~ and BS: ~~84~~ BS: 98 % during BS: ~~winter~~ BS: post monsoon season.

Long range transport was responsible for both, bringing air masses with a significantly lower fraction of exceedance days from the Eastern IGP and air masses with a moderate increase in the fraction of exceedance days from the West (Source region: Arabia, Thar desert, Middle East and Afghanistan).

In order to bring PM mass loadings in compliance with the BS: ~~national ambient air quality standard (NAAQS)~~ NAAQS and reduce the number of exceedance days, mitigation of regional BS: ~~pollution~~ combustion sources in the NW-IGP needs to be given highest priority.

1 Introduction

India is a rapidly developing nation. Population growth, urbanization and industrial development have led to increasing emissions, resulting in particulate matter (PM) mass loadings that frequently exceed the national ambient air quality standard (NAAQS) of 100 µg m^{-3} for 24 h average PM_{10} and 60 µg m^{-3} for 24 h average $PM_{2.5}$ mass loadings. This exposes the residents to hazardous levels of PM throughout the year.

Daily particulate matter mass loadings show a clear correlation with daily mortality and morbidity from respiratory and cardio vascular diseases (Englert, 2004; Kappos et al., 2004;

Pope and Dockery, 2006). The correlation between extreme PM mass loadings and mortality has been recognized early in the history of air pollution research (Firket, 1931; Schrenk et al., 1949; Nemery et al., 2001) and the predicted disaster of the "London Fog" (Logan, 1953; Bell and Davis, 2001) resulted in first efforts to combat PM air pollution through legislation and regulatory intervention. However, the effect of moderate to low PM mass loadings on human health was recognized much later (Shy, 1979; Ware et al., 1981; Dockery et al., 1989, 1993; Schwartz, 1994; Pope et al., 1995; Pope, 2000) and the accumulated evidence has resulted in a revision of the air quality standards in many countries including India (NAAQS, 2009).

Many sites in the densely populated IGP are in violation of the NAAQS throughout the year except during the monsoon season, when removal through wet scavenging brings PM levels into compliance. Enhanced PM is associated with increased hospital visits/admission of patients with respiratory symptoms and increased mortality (Mohanraj and Azeez, 2004; Nag et al., 2005; Pandey et al., 2005; Kaushik et al., 2006). The complex interplay of natural windblown dust, trans-boundary air pollution and local sources impose severe challenges on the Central Pollution Control Board, the local regulatory body in charge of enforcing the NAAQS. While it is clearly inappropriate to blame individual industrial units for natural windblown dust or trans-boundary air pollution, the contribution of these two factors to extreme events should not be used as an excuse to avoid all regulatory action. This study seeks to quantify the effect of long range transport of both natural windblown dust and anthropogenic PM to the regional background PM mass loadings and to establish a baseline against which the enhancement due to local sources can be measured.

Back trajectory models use archived meteorological data and allow for the identification of source regions of pollutants measured at a receptor site. Air mass trajectories are defined as the path of an infinitesimally small air parcel. Back trajectories trace the air mass back in time and describe where the air mass reaching a receptor site originated.

Statistical analysis of large datasets BS: ~~of air mass back trajectories~~ has been a popular tool for identifying source regions of particulate matter. Such BS: ~~statistical~~ analysis attributes all changes in particulate matter mass loading at a receptor site to spatially fixed sources and

seeks to identify those sources by investigating the statistical correlation between air mass origin and the particulate mass loadings observed at the receptor site. While wind rose or pollution rose plots are most appropriate to identify local sources (Fleming, 2012), BS: ~~statistical~~ analysis of a large set of back trajectories (Stohl, 1996, 1998) has been a popular tool for identifying distant source regions of particulate matter (Borge et al., 2007; Abdalmogith and Harrison, 2005; Nyanganyura, 2008; Buchanan et al., 2002) and investigating trans-boundary particulate matter pollution (Miller et al., 2010; Grivas et al., 2008; Borge et al., 2007). Cluster analysis is a multivariate statistical technique that splits the data into a number of groups while maximizing the homogeneity within each group and maximizing the distance between groups.

The aim of the present study is to better understand the conditions under which PM mass loadings exceeding the national ambient air quality standard (NAAQS) of 100 $\mu g\,m^{-3}$ for 24 h average PM_{10} and 60 $\mu g\,m^{-3}$ for 24 h average $PM_{2.5}$ (NAAQS, 2009) occur in the North West Indo Gangetic Plain (NW-IGP) and to quantify the contribution of long range transport to those exceedance events. Here, we quantify the contribution of long range transport to fine ($PM_{2.5}$) and coarse ($PM_{10-2.5}$) particulate matter (PM) using back trajectory cluster analysis, pinpoint potential source regions of enhanced background PM mass loadings and further attempt to constrain the origin of the particulate matter by correlating the observations with those of gas phase combustion tracers (CO, NO_2, benzene and acetonitrile). We analyse a two year dataset (August 2011 till June 2013) measured at the Atmospheric Chemistry facility of the Indian Institute for Science Education and Research (IISER) Mohali.

2 Materials and methods

2.1 Study location, air quality data and general meteorology

We use two years (August 2011 till June 2013) of hourly data of fine ($PM_{2.5}$) and coarse ($PM_{10-2.5}$) particulate matter (PM) and gas phase combustion tracers (CO, NO_2, benzene

and acetonitrile) measured at the Atmospheric Chemistry facility of the Indian Institute of Science Education and Research Mohali. The facility, the measurement techniques used, data coverage and data quality assurance protocols are described in great detail in Sinha et al. (2014), hence only a brief description is provided here. Particulate matter (PM_{10} and $PM_{2.5}$) mass concentrations were measured using separate Thermo Fischer Scientific 5014i beta continuous ambient particulate monitors working on the principle of beta attenuation, NO_2 measurements were performed by chemiluminescence technique using a Thermo Fischer Scientific 42i trace level analyser, Carbon monoxide (CO) was measured by gas filter correlation (GFC) non dispersive infrared (NDIR) technique using Thermo Fischer Scientific 48i trace level enhanced analyser and the mixing ratios of benzene and acetonitrile were determined using a high sensitivity proton transfer reaction quadrupole mass spectrometer (HS Model 11-07HS-088; Ionicon Analytik Gesellschaft, Austria). *BS:* The inlets of all instruments and the meteorological sensors are co-located and placed at a measurement height of 20 m a.g.l (Sinha et al., 2014).

Figure 1 shows the location of city Mohali in the north-west Indo-Gangetic plain in the Indian state Punjab, close to the forested slopes of the foothills of the Himalayan mountain range on the left side. The measurement facility is located at a suburban site, south west of the city centre of the "tri-city" – an urban agglomeration of the three cities Chandigarh, Mohali and Panchkula – inside the residential campus of IISER Mohali (30.667° N, 76.729° E, 310 m a.m.s.l.). On the right side, Fig. 1 shows a close up illustrating the exact location of the measurement facility and its spatial relationship with respect to the nearby cities and potential local point sources of particulate matter and the mountain range.

Figure 2 shows wind rose plots for winter (December–February), summer (March–June), monsoon (July–September) and post-monsoon (October and November) season. Most air masses impacting the site travel parallel to the mountain range and reach the facility from north-western or south-eastern direction. Periods of calm (wind speed $< 1\,m\,s^{-1}$) account for only 4.5, 2.5, 5.2 and 8.7 % of the total time during winter, summer, monsoon, post-monsoon season respectively and slow transport (wind speed 1–5 $m\,s^{-1}$) was observed 64.1, 48.7, 56.1 and 71.4 % of the total time, respectively. The high frequency with which

rapid transport of air masses towards the facility (wind speed $> 5\,\mathrm{m\,s^{-1}}$) was observed (31.4, 48.8, 38.7 and 19.9 % of the total time during winter, summer, monsoon, post-monsoon season respectively) indicates that long range transport potentially plays a significant role in determining pollutant loadings at the site. The general meteorology of the site is as follows.

During winter season, weak northerlies or north-westerlies and a weak, low-level anticyclonic circulation prevails in the NW-IGP. BS: The surface pressure map, the surface winds and 700 hPa winds of NCEP Reanalysis derived data provided by the NOAA Physical Science Division, Boulder, Colorado, USA are shown in supplementary Figure 1 panels a)–c). Wintertime fog occurs frequently and is favoured by subsidence of air masses over the IGP, low temperatures, high relative humidity and low wind speeds ($< 5\,\mathrm{m\,s^{-1}}$). BS: However, ground level wind speeds at our site are generally not as low as the surface wind speeds of the NCAR Reanalysis dataset would suggest. The seasonally averaged experimentally observed wind speed is 4.4 $\mathrm{m\,s^{-1}}$ BS: and not $< 2\,\mathrm{m\,s^{-1}}$ BS:. This underestimation of the surface wind speeds in the NW-IGP is not unique to this particular model and meteorological dataset but also applies to e.g. Figure 6 in Lawrence and Lelieveld (2010). Sporadic winter rains are generally associated with the western disturbance (Pisharoty and Desai, 1956; Agnihotri and Singh, 1982; Mooley, 1957; Dimri, 2004). The western disturbance is a terrain-locked low-pressure system that forms when an upper-level extra tropical storm originating over the Mediterranean passes over the notch formed by the Himalayas and Hindu Kush mountains. The resulting notch depression is small, five degrees latitude/longitude in size, and develops within an existing trough in the belt of subtropical westerly wind. South-westerly wind ahead of the trough brings moisture from the Arabian Sea, which encounters the Western Himalayas that lie almost normal to this moist wind. Part of the wind is channelled into the IGP which subsequently reach the receptor site from the southeast. Fast westerly winds in winter are typically associated with a strong subtropical jet stream poised over westerly troughs.

During summer season, the prevailing wind direction is north-westerly. Tropospheric subsidence over north-western India due to the “heat low” associated with westerly flow across

Afghanistan and Pakistan, channels air masses originating in the Middle East into the IGP BS: (Supplementary Figure 1 pannels d-f). The boundary layer, experiences a strong temperature inversion (Das, 1962) due to dust induced cooling in the upper layers. The resulting steep horizontal pressure gradient is responsible for strong surface winds that carry dust and sand storms (Bryson and Swain, 1981). These loo-winds are extremely hot and dry BS: and are not adequately resolved by the NCEP Reanalysis meteorological dataset (Supplementary Figure 1, pannels d-f), which shows a very moderate average surface wind speed of 1.5-2.5 $\mathrm{m\,s^{-1}}$ BS: over the NW-IGP that stands in stark contrast to the observed seasonally average wind speed of 5.6 $\mathrm{m\,s^{-1}}$. During April, the centre of the subtropical jet stream is located over Northern India and gives rise to cold subtropical westerlies in the upper troposphere. At the same time the lower troposphere reaches very high temperatures due to quick response of the land to the overhead sun. This favours severe thunderstorms with strong squalls at the leading edge of the downdraft during summer season. Such thunderstorms can cause convective dust storms, locally known as "Aandhi" (Ramaswamy, 1956; Joseph, 1982). In March and April, south-easterly winds are generally associated with the western disturbance. The climatology of the western disturbance shows a significant inter-annual variability, as it is correlated with the Polar/Eurasia tele-connection pattern. A weak circumpolar vortex can lead to an enhancement in the number of notch depressions and late "winter storms" in March and April (Lang and Barros, 2004). South-easterly winds in June are generally associated with an earlier than usual onset of the monsoon. In normal years the monsoon reaches Punjab in the first week of July.

During monsoon season, the surface heat low located over the Pakistan region and the monsoon trough stretching from the North-West IGP to the Bay of Bengal dominate the general circulation over the IGP BS: (Supplementary Figure 1, pannels g-i). The strength and position of the monsoon trough drives the "active-break" cycles of the rains on the intra-seasonal scale (Sikka and Gadgil, 1980; Goswami, 1998; Goswami et al., 2006a, b). During "active" spells the trough is located over south or central India and cyclonic swirls form all across the trough. The prevailing wind direction during active spells is south-easterly. During "break" spells the trough is located over the foothills of the Himalayas, the low level

jet originating off the coast of Somalia enters the IGP through the Indus valley (Joseph and Raman, 1966). Cyclonic swirls are mostly absent and rains are suppressed everywhere except over the foothills (Joseph and Sijikumar, 2004). During break spells of the monsoon circulation, the prevailing wind direction is north westerly. Break spells are associated with lower-tropospheric inversions, dusty winds and lower troposphere anti-cyclonic vorticity over the IGP (Sikka, 2003; Rao and Sikka, 2005; Bhat, 2006). BS: Both the observed wind direction and wind speeds of the surface winds during monsoon season are poorly resolved by the meteorological dataset. While the model suggests low wind speed ($<2\,\mathrm{m\,s^{-1}}$ BS: south westerly winds dominate (Supplementary Figure 1 pannels g-i), actual observations show that north westerly winds dominate during break spells and south easterly winds during active spells. The average wind speed is 5.1 $\mathrm{m\,s^{-1}}$. Most rainfall events occur during the "active spells" when the wind direction is south-easterly. However, occasional night time rainfall events are observed even during break spells in Punjab.

During post monsoon season, the prevailing wind direction is north-westerly. The retreating monsoon brings subsidence of dry Central Asian air masses over the North-west IGP. In particular during night time, katabatic winds reach the receptor site from the northern to eastern wind sector. Winds are generally weak; the wind speed is less than $5\,\mathrm{m\,s^{-1}}$ for more than 80 % of the time. BS: Post monsoon season shows the lowest discrepancy between modelled surface winds 1.5-2 $\mathrm{m\,s^{-1}}$ BS: and observed wind speeds 3.4 $\mathrm{m\,s^{-1}}$ BS: (Supplementary figure 1, panel j-l). Surface wind vectors represent the observed night time flow at our site better, while the 700 ha Pa wind vectors represent daytime observations better.

Since the purpose of this study is to investigate the contribution of long range transport to PM pollution we restricted our analysis to measurements obtained between 12 BS: noon to 4 p.m. LT (UTC + 05:30) during the day and 3 to 6 a.m. LT (UTC + 05:30) at night BS: as depicted in Fig. 3 and consider calm conditions with wind speeds of less than $1\,\mathrm{m\,s^{-1}}$ separately.

The daytime period was selected, because the local daytime boundary layer reaches its maximum height around 2 p.m. and the contribution of long range transport to PM is highest in the time period centred on this time.

The night time period was selected because the contribution of local sources, in particular the contribution of local traffic, construction activity and biomass combustion to air pollution is least during late night and early morning hours.

Figure 3 shows that both fine mode PM ($PM_{2.5}$, bottom panels) and coarse mode PM ($PM_{10-2.5}$, top panels) show a bimodal distribution with a peak in the morning and the evening due to local traffic and biomass combustion emissions and a low in the mid-day hours and the early morning hours during all seasons (Fig. 3). The bimodal behaviour is most pronounced during post monsoon season, when low wind speeds prevail and local and regional sources dominate the aerosol mass loading. The bimodal behaviour is weakest during monsoon season when active convection and high wind speeds reduce the influence of local sources. Fine mode PM shows the lowest mass loadings during mid-day, when the boundary layer is highest, while coarse mode PM shows the lowest mass loadings in the early morning hours.

During summer and monsoon season, there is a pronounced difference between mean and median coarse mode PM loadings. This discrepancy is caused by the contribution of episodic events (dust storms) to coarse mode PM in both seasons. For our back trajectory analysis, we calculated the median PM mass loading (see the Supplement) and gas phase mixing ratio of CO, benzene and acetonitrile for the period in question. For rainfall we provided the sum (total precipitation in the time window in question) rather than the median, as we consider the total rainfall a better indicator of wet scavenging.

2.2 Back trajectory modeling

We computed three day (72 h) backward trajectories using HYSPLIT_ 4 (HYbrid Single Particle Lagrangian Integrated Trajectory) model in ensemble mode using National Oceanic and Atmospheric Administration's BS: ~~Global Data Acquisition System~~ **G**lobal **D**ata **A**cquisition **S**ystem BS: (GDAS) meteorology (Draxler and Rolph, 2013; Draxler and Hess, 1998) as in-

put. We calculated ensemble runs for air masses arriving at the site (30.667° N, 76.729° E) at 20 m above the ground (the approximate sampling height for all instruments). The model was run twice daily with an arrival time of 09:00 UTC (2.30 p.m. local day-time) and 23:00 UTC (4.30 a.m. local night-time). Due to the close proximity of the site to the Himalayan mountain range the trajectory output was found to be very sensitive to the model's input data. IISER Mohali Air Quality station (30.667° N, 76.729° E) is located in the Indo-Gangetic Plain (IGP) at an altitude of 310 m a.m.s.l. approximately 20 km south west of the Shivalik hills, but the model's terrain height at the receptor site is 667.6 m a.m.s.l. for the GDAS BS: ~~dataset~~meteorological data field and 1249.9 m a.m.s.l. for the reanalysis BS: ~~dataset~~meteorological data field for a single trajectory arriving at the site. We calculated trajectory ensembles for our site using both datasets. The trajectory ensemble option starts multiple trajectories from the selected starting location. Each member of the trajectory ensemble is calculated by offsetting the meteorological data by a fixed grid factor (1 meteorological grid point in the horizontal and 0.01 sigma units in the vertical) which results in 27 trajectories. The model's terrain height varied between 200 and 3500 m a.m.s.l. for individual runs of the trajectory ensemble for the GDAS BS: ~~dataset~~meteorological data field and between 240 and 5100 m a.m.s.l. for the reanalysis BS: ~~dataset~~meteorological data field . We conclude that the GDAS BS: ~~dataset~~meteorological data field performs better in modelling the terrain at our site and all further analysis in this work uses this BS: ~~dataset~~meteorological data field .

Out of the 27 trajectories in the ensemble run, only 3 trajectories are consistent with the measurement site, Mohali, being located in the plain ($<$ 400 m a.m.s.l.) and Shimla, a mountain site 60 km NE of our site (Fig. 1) at 31.103° N, 77.172° E, being located in the mountains ($>$ 400 m a.m.s.l.). BS: To ensure that this sensitivity of the model does not affect the results of our study, we selected these three trajectories for further analysis.

Borge et al. (2007) have recently emphasised the importance of specifying adequate arrival heights for the outcome due to possible large variation in the wind speed and direction with height above the ground. Kassomenos et al. (2010), too, found a dependency of clustering outcome on the arrival heights of the trajectories. At our site, we find that

the Himalayan mountain range acts as a great barrier and air masses are funnelled into the IGP. Consequently there is little dependency of the trajectory run outcome on arrival heights ≤ 500 m a.g.l., as long as the meteorological input data set represents the Himalayan mountain range topography adequately. The local wind direction observed at the site generally agrees with the wind vector at 10 m a.g.l. used in the GDAS *BS:* ~~dataset~~meteorological data field .

2.3 Back trajectory cluster analysis

Cluster analysis is a statistical method used to group data in large data sets into a small number of groups of similar data known as clusters. In this work we have used air masses' trajectory coordinates (time steps) as the clustering variables. A non-hierarchical method known as the k means procedure has been used in this study. The air mass back trajectories were subjected to k means clustering using a freeware called PAST (PAleontological STatistics). The number of clusters "k" is to be specified by the user prior to clustering. The assignment of back-trajectories to clusters is initially random. In an iterative procedure, trajectories are then moved to the cluster which has the closest cluster mean in Euclidean distance, and the cluster means are updated accordingly (Bow, 1984). This process continues until the process of hopping from one cluster to another ceases. As a normal artefact of the k means clustering algorithm, the result is dependent upon the seed used for clustering (Kassomenos et al., 2010). Therefore, to get a robust result, clustering was initialized with 11 different trajectory orders and we selected the clustering result with the lowest root mean square difference for each predefined number of clusters.

The root mean square difference for an individual latitude and longitude value is given by

$$\text{RMSD} = \sqrt{(x_i - \bar{x})^2} + \sqrt{(y_i - \bar{y})^2} \quad (1)$$

where x_i and y_i stand for the latitude and longitude of the individual trajectory for a given hour and $\bar{x}$ and $\bar{y}$ for the cluster mean latitude and longitude of the same hour for the cluster to which that trajectory belongs. The total root mean square difference t-RMSD is the sum over all the RMSD values for a given set of back trajectories.

We selected the optimal number of clusters that best describe the different air–flow patterns to our site by computing the change in the minimum t-RMSD while increasing the number of clusters from n to $n+1$. This change in the minimum t-RMSD decreases abruptly as clusters of trajectories which are significantly different in terms of wind directions and speeds are separated from each other (Dorling et al., 1992). A threshold of 5 % change has been adopted (Brankov et al., 1998; Dorling et al., 1992) as an indication of the number of clusters to be retained.

3 Results and discussions

3.1 Optimization of the number of clusters

The number of clusters was optimized by minimizing the t-RMSD change for an increase in number of clusters, while retaining as few clusters as possible. [BS:] Supplementary Figure 2 shows the percent change in t-RMSD for a subsequent increase in number of clusters. The largest % decrease in t-RMSD is observed when the number of clusters is increased to 2 and subsequently 3. This corresponds to two major airflow corridors (southeasterly flow and westerly flow) and a local cluster. Increasing the number of clusters beyond this number allows splitting of the air masses in the western and southeastern corridor into several groups according to their transport speed and introduces a south westerly cluster. Initially, we identified the optimum number of clusters as seven, however, two of these seven clusters (fast north-westerly flow A and B) were classified into two different groups only, because for fast north-westerly flow “A” all three trajectories of the ensemble run showed equal transport speed while for fast north-westerly flow “B” two of the three trajectory solutions in the ensemble indicated slow air mass transport (trajectories arriving at 20 m a.g.l., [BS:] Supplementary Figure 3) while one solution supported rapid transport (trajectory arriving at 250 m a.g.l., [BS:] Supplementary Figure 3). Locally measured meteorological parameters indicated that both clusters are associated with hot dry “loo-winds” and dust storms during summer and above average wind speeds during other seasons. Therefore, both clusters

were combined into one fast westerly cluster and the final number of optimum clusters was 6.

3.2 Spatial and dynamic patterns of the air flow associated with the clusters

Figure 4 shows the BS: ~~average~~ trajectories of BS: of the cluster averages and individual trajectories associated with each cluster BS: ~~seven clusters~~ identified by k means clustering superimposed on a land classification map (courtesy ESA GlobCover 2009 Project). The length of each mean trajectory is 3 days and the distance between two successive data points represents the 1 h interval. We find six distinct flow patterns, south easterly flow ($N = 263$), south westerly flow ($N = 79$), fast ($N = 78$), medium ($N = 83$) and slow ($N = 305$) westerly flow and a local cluster ($N = 556$). BS: ~~Figure 7a–f shows all the individual trajectories that contributed to each of the clusters, superimposed on a land classification map (courtesy ESA GlobCover 2009 Project). These plots give a qualitative impression of the variability of the flow within the individual clusters.~~ Although considerable variability is observed between the individual trajectories contributing to each of the clusters, in particular for the "local" cluster, each cluster of trajectories represents a distinct air mass fetch region. BS: Supplementary Figure 3 depicts the mean height (m a.g.l.) of the mean trajectories during the three days before their arrival at the receptor site. Trajectories from the slow, medium and fast westerly clusters descend from the free troposphere to reach the receptor site. Fast and medium westerly air masses show a rapid descent in the last 30 h prior to reaching the receptor site and are generally associated with high wind speeds, while slow westerly air masses display a gradual subsidence. The south easterly, south westerly and local cluster remain within the convective boundary layer throughout.

Figure 5 shows the temporal distribution of the air flows for the six clusters determined with respect to the different seasons and Table 1 presents the locally measured meteorological parameters for daytime/nighttime for each cluster and season. BS: A detailed description

of the meteorological conditions and synoptic scale air mass flow associated with each of the clusters can be found in the supplementary text.

BS: The *local cluster* accounts for 40.1, 35.7, 31.1 and 51.3 % BS: of the air mass trajectories during winter (December to February), summer (March to June), monsoon (July to September) and post-monsoon (October and November) season respectively. This air mass transport corresponds to times when weak northerlies or north-westerlies and a weak, low-level anti-cyclonic circulation prevail in the NW-IGP during winter, summer and post monsoon season. The predominant locally measured wind direction for this cluster during winter, summer and post monsoon season is west to north-west (47 % BS: of the time) with katabatic winds (320–120° BS: wind sector) accounting for most of the remainder (31 % BS:). South easterly winds (8 % BS:) and south westerly winds (14 % BS:) account only for a minor fraction of the locally observed wind direction each. During summer season and monsoon season convective activity above the site is also attributed to this cluster. Strong squalls leading to "Aandhi" type convective dust storms (Joseph, 1982) BS: are observed occasionally, both in late summer and early in the monsoon season. During monsoon season, locally observed wind direction associated with this cluster is variable (35 % BS: north west, 29 % BS: south east, 18 % BS: south west, 18 % BS: katabatic flow). The local cluster is associated with average temperatures and wind speeds at the lower end of those observed for the different clusters both during day and night in all seasons. The absolute humidity is higher than the absolute humidity observed for medium and fast westerly flows and lower than the absolute humidity observed for south easterly and south westerly flow during all seasons. Occasionally rain events occur in all seasons, however, the total number of rain events associated with the local cluster is low except during monsoon season.

The *slow westerly* cluster is associated with the same general meteorology (weak northerlies or north-westerlies and a weak, low-level anti-cyclonic circulation) as the local cluster and most of the locally observed parameters are also similar to those of the local cluster. However, the fetch region of the air masses is larger. The predominant local wind direction for this cluster is west to northwest during all seasons including monsoon (50 % BS:) and katabatic winds from the north-northwest to east-southeast sector (28 % BS:) account for most of the remainder. South easterly winds (10 % BS:) and south westerly winds (12 % BS:) account only for a minor fraction of the locally observed wind direction each. The main differences between air masses associated with the local cluster and air masses associated with the slow westerly cluster are as follows: slightly higher temperatures and wind speeds are observed for the slow westerly cluster during most seasons and both relative and absolute humidity are lower for air masses associated with the slow westerly cluster due to the re-

cent descend of the air masses from the free troposphere. Air masses associated with the slow westerly cluster have a shorter residence time in the convective boundary layer over the irrigated fields in the IGP and consequently contain less moisture. The slow westerly cluster accounts for 17.4, 26.6, 10.7 and 28.4 %$^{BS:}$ of the air mass transport to the site during winter, summer, monsoon and post-monsoon season respectively. Rain events are associated with this cluster only rarely.

The *medium westerly* cluster is observed only during winter, summer and post monsoon seasons and accounts for 7.7, 8.5 and 4.5 %$^{BS:}$ of the air masses respectively. The clusters are associated with a strong subtropical jet stream poised over westerly troughs and shows higher than average wind speeds. The predominant local wind direction for this cluster is west to northwest during all seasons (44 %$^{BS:}$) and katabatic winds from the north-northwest to east-southeast sector (38 %$^{BS:}$) account for most of the remainder of the flow. South westerly (13 %$^{BS:}$) and south easterly winds (6 %$^{BS:}$) account for only a minor fraction of the locally observed wind direction each. Air masses associated with this cluster descended from the free troposphere less than 30 h$^{BS:}$ prior to their arrival at the receptor site and had significant residence time over arid regions west of India. Consequently, they are associated with low relative and absolute humidity and do not bring rain. The medium westerly cluster is typically observed shortly before the arrival of a western disturbance.

The *fast westerly* cluster is observed only during winter, summer and post monsoon seasons and accounts for 7.7, 6.4 and 6.4 %$^{BS:}$ of the air masses respectively. The cluster is associated with a strong subtropical jet stream poised over westerly troughs and shows higher than average wind speeds. The predominant local wind direction for this cluster is West to Northwest during all seasons (60 %$^{BS:}$) and katabatic winds from the north-northwest to east-southeast sector (30 %$^{BS:}$) account for most of the remainder. South westerly (6 %$^{BS:}$) and south easterly winds (4 %$^{BS:}$) account only for a minor fraction of the locally observed wind direction each. Due to the fact that air masses associated with this cluster descended from the free troposphere less than 30 h$^{BS:}$ prior to their arrival at the receptor site and had significant residence time over arid regions west of India, they are associated with low relative and absolute humidity and do not bring rain. The fast westerly cluster is most frequently observed during winter and early summer season 2–3 days$^{BS:}$ prior to the arrival of a western disturbance.

The *south easterly* cluster is associated with the passage of a western disturbance in winter and summer and with active spells of the monsoon during monsoon season and accounts for 19.3, 13.1 and 42.6 %$^{BS:}$ of the flow respectively. It is generally not observed during post monsoon season. The western disturbance is responsible for most of the wintertime and summer time rain events (Table 1). During winter and summer season, the predominant local wind direction for this clus-

ter is south easterly (38 %$^{BS:}$). Katabatic winds from the north-northwest to east-southeast sector account for 27 %$^{BS:}$, south westerly winds for 17 %$^{BS:}$ and north westerly winds for 18 %$^{BS:}$ of the locally observed wind direction. Temperatures and wind speeds associated with this cluster are above average in winter and below average in summer. The relative and absolute humidity of air masses associated with this cluster are always high during both seasons. During monsoon season, the "Bay of Bengal branch" of the monsoon circulation brings warm and moist air masses to the receptor site. The absolute humidity is high and the highest total amount of rainfall is observed for this cluster. The predominant local wind direction for this cluster is south east (53 %$^{BS:}$). Katabatic winds from the north-northwest to east-southeast sector account for 24 %$^{BS:}$, south westerly winds for 12 %$^{BS:}$ and north westerly winds for 11 %$^{BS:}$ of the locally observed wind direction.

The *south westerly* cluster is associated with the passage of a western disturbance in winter and summer and with "break" spells of the monsoon during monsoon season and accounts for 3.4, 7.3 and 10.4 %$^{BS:}$ of the flow respectively. It is not observed during post monsoon season. During winter and summer, the south westerly cluster is usually observed in association with a weakening western disturbance or at times when the centre of the low pressure system is above or close to the receptor site. The predominant local wind directions are west to northwest (42 %$^{BS:}$) and southeast (35 %$^{BS:}$). South westerly winds (13 %$^{BS:}$) and katabatic flow (10 %$^{BS:}$) account only for a minor fraction of the locally observed wind direction. During monsoon this cluster is associated with "break" spells. "Break" spells occur when the monsoon trough is located over the foothills of the Himalayas and the low level jet originating off the coast of Somalia enters the IGP through the Indus valley. The local wind direction is variable: 46 %$^{BS:}$ south east, 21 %$^{BS:}$ north west 21 %$^{BS:}$ katabatic flow and 11 %$^{BS:}$ south westerly winds. The absolute humidity of air masses associated with this cluster is high although rainfall events occur only rarely. However, extreme rainfall events are associated more frequently with this cluster.

Calm conditions (WS $< 1\ \mathrm{m\,s^{-1}}$ $^{BS:}$) account for only 4.5, 2.5, 5.2 and 8.7 %$^{BS:}$ of the total time during winter, summer, monsoon, post-monsoon season respectively. They occur more frequently at night (60 %$^{BS:}$) and less frequently during the day (40 %$^{BS:}$). The local wind direction during periods with low wind speed is variable: 36 %$^{BS:}$ south west, 33 %$^{BS:}$ katabatic flow, 19 %$^{BS:}$ south east and 12 %$^{BS:}$ north west.

3.3 Impact of air mass transport on Particulate Matter (PM) mass loadings

To quantify the contribution of long range transport to particulate matter mass loadings at the receptor site we calculated the cluster average mass loadings of coarse and fine mode particulate matter at the receptor site (Fig. 6) and the enhancement of PM mass loadings above the levels observed for the "local" cluster which represents the regional background pollution in the North West IGP best (Table 2). The enhancement is expressed in % of the total PM mass loading observed for the respective cluster. We determined whether the differences in PM mass loadings between the different clusters are significant using Levene's test for homogeneity of variance based on means and used the pair wise comparison based on Tukey's studentised HSD test (Honestly Significant Differences) for assessing the statistical significance of the difference of the mean for each pair of clusters and each season (Table 3).

3.3.1 Winter season

During winter season both long range transport from the west and south west and local pollution episodes lead to enhanced coarse mode PM mass loadings (Table 2). The contribution of long range transport to coarse mode particulate mass loadings varies from 9 % for the south westerly cluster to 28 % for the medium westerly cluster. Local pollution episodes contribute 14 % on an average to the coarse mode PM observed under calm conditions.

Despite the fact that the average coarse mode PM varies from 45 $\mu g\,m^{-3}$ for the south easterly cluster to 66 $\mu g\,m^{-3}$ for the medium westerly cluster BS: ~~(Table 3)~~ (BS: Fig. 6) the difference of the average is not statistically significant for any of the cluster pairs due to the high intra-cluster variance of coarse mode PM during winter season (BS: Table 3). BS: ~~Two sources contribute prominently to coarse mode PM mass loading during winter: aqueous phase oxidation of gas phase precursors and dust.~~ Figure 7 shows the correlation of CO with coarse mode PM ($PM_{10-2.5}$) as a function of meteorological conditions. BS: It can be seen from this figure that two sources contribute prominently to coarse mode PM mass loading during winter: aqueous phase oxidation of gas phase precursors and dust. Aqueous phase oxidation of

gas phase precursors refers to a process wherein gases (e.g. NH_3(g), SO_2(g), NO_2(g))[BS: are taken up by aqueous phase aerosol and subsequently undergo reactions that change the oxidation state resulting in the formation of ammonium, sulphate and nitrate ions. Upon drying these precipitate out as salts which can be of coarse mode in size.] Aqueous phase oxidation of gas phase precursors emitted during combustion leads to a high degree of correlation between coarse mode particulate matter and CO at high relative humidity ($> 70\,\%$, $r = 0.55$), while dust, both dust from long range transport and locally suspended dust, contributes significantly to coarse mode PM at RH $< 50\,\%$ and high wind speeds (Fig. 7). The complex interplay of meteorology dependent emissions and oxidation leads to high intra-cluster variance of PM mass loadings and obscures the contribution of long range transport to PM levels.

The influence of wet scavenging on PM mass loadings, however, is statistically significant. During rain events, coarse mode PM mass loadings drop to $30\,\mu g\,m^{-3}$ under calm conditions ($-47\,\%$), $13\,\mu g\,m^{-3}$ for the local cluster ($-72\,\%$) and $11\,\mu g\,m^{-3}$ for the south easterly cluster ($-78\,\%$) and the magnitude of the drop depends only weakly on the total amount of rainfall. Fine PM mass loadings drop to $73\,\mu g\,m^{-3}$ under calm conditions ($-48\,\%$), $80\,\mu g\,m^{-3}$ for the local cluster ($-27\,\%$) and $15\,\mu g\,m^{-3}$ for the south easterly cluster ($-80\,\%$). This clearly demonstrates the profound influence of wet scavenging on fine mode PM mass loadings during winter. The percent decrease in fine mode PM mass loadings during rain events scales perfectly linearly with the total rainfall for each cluster (1.3 % decrease in $PM_{2.5}$ per mm of rainfall, $r^2 = 0.99$). The fact that the drop in coarse mode PM is independent of the total amount of rain while the drop in fine mode PM strongly depends on the total amount of rainfall could be an indicator that during winter time, soluble coarse mode PM (large salts) plays a crucial role in initiating rainfall as giant cloud condensation nuclei, while fine mode PM is mostly scavenged by below cloud scavenging.

For fine mode PM, local pollution episodes lead to the highest enhancements in fine mode PM mass loadings (22 %). Long range transport from the west contributes only moderately to fine mode PM (7 and 13 % for the medium westerly and slow westerly cluster respectively).

The highest fine mode PM mass loadings are observed under calm conditions during local pollution episodes (141 $\mu g\,m^{-3}$). The enhancement is significant when compared to the south-easterly (72 $\mu g\,m^{-3}$) south westerly (101 $\mu g\,m^{-3}$) and fast westerly cluster (100 $\mu g\,m^{-3}$). When only dry days are considered, the difference between local pollution episodes (146 $\mu g\,m^{-3}$ on dry days) and the local cluster (110 $\mu g\,m^{-3}$ on dry days), which represents the regional air pollution also becomes significant (Table 3).

The lowest fine mode PM mass loadings are observed for the south-easterly cluster (72 $\mu g\,m^{-3}$) – which is associated with the western disturbance and has significantly lower mass loadings than the local, slow westerly and medium westerly cluster. The fast westerly cluster which is usually observed shortly before a western disturbance establishes itself over India has the second lowest fine mode mass loadings (100 $\mu g\,m^{-3}$), though the difference is not statistically significant with respect to the other clusters due to large intra-cluster variability in the fine mode PM mass loadings.

During winter-time, emission of fine mode particulate matter is driven by combustion. Correlation plots of fine PM with CO ($r^2 = 0.70$), acetonitrile, a biomass combustion tracer ($r^2 = 0.35$), benzene ($r^2 = 0.49$) and NO_2, a tracer for high temperature combustion, ($r^2 = 0.43$), Fig. 8) clearly indicate that at the receptor site combustion is the predominant source of winter time fine mode PM across all clusters. Due to low ambient temperatures in the winter months, in particular in the surrounding mountain regions, those who cannot afford electric heaters burn dry leaves, wood, coal, agricultural residues and cow dung often mixed with garbage to keep themselves warm. This practice prevails in entire South Asia and explains the simultaneous increase in fine mode PM and acetonitrile during winter season. High emissions of benzene have previously been observed during biomass combustion episodes in the region (Sarkar et al., 2013) and inefficient combustion in open fires or simple stoves is known to cause high PM mass loadings (Habib et al., 2004; Venkataraman et al., 2005; Massey et al., 2009; Akagi et al., 2011). While there is a clear correlation between both benzene and acetonitrile and $PM_{2.5}$, the lower r^2 for acetonitrile ($r^2 = 0.35$) compared to the higher r^2 for benzene ($r^2 = 0.49$) and CO ($r^2 = 0.70$) indicates that mixtures of fuels with variable biomass content are used for domestic heating purposes. The scatter plot

between $PM_{2.5}$ and benzene (Fig. 8) also seems to suggest that there may be regional preferences with respect to the fuel mixture as the emission ratios of the south easterly cluster usually fall below the fit line, while those for the south westerly cluster fall above it. The largest scatter and hence variation in fuel type is observed under calm conditions and for the local and slow westerly cluster.

The high mass loading of fine mode particulate matter coupled with the high relative humidity, which frequently reaches values above 75 %, in particular during the night, leads to the formation of persistent fog and haze during winter time. The uptake of water soluble organic and inorganic gas phase species into the aqueous phase and the subsequent chemical reactions result in a fine mode aerosol that contains a large mass fraction of water soluble inorganic species (Kumar et al., 2007) and acts as a very efficient CCN. Repeated fog processing also leads to the formation of coarse mode inorganic salt particles (Kulshrestha et al., 1998; Kumar et al., 2007). Kaskaoutis et al. (2013) reported a bi-modal volume size distribution for wintertime aerosol in Kanpur with a first, higher peak between 200–300 nm and a second peak between 3–4 µm optical equivalent diameter. The ratio of coarse mode to fine mode PM observed at our site agrees well with the ratio of coarse mode to fine mode PM observed in their study. Kulshrestha et al. (1998) reported a bimodal size distribution peaking at 1 and 5 µm aerodynamic equivalent diameter for wintertime aerosol in Agra and found ammonium sulphates, ammonium nitrate and potassium sulphate dominated water soluble salts in the fine mode while sulphates, nitrates and chlorides of sodium, calcium and magnesium dominated coarse mode aerosol. Dey and Tripathi (2007) reported that in wintertime in Kanpur more than 75 % of coarse mode particulate matter consisted of water soluble salts and only less than 25 % of coarse mode PM consisted of mineral dust. Their findings are in line with our observations that aqueous phase processing of gas phase precursors is responsible for a significant fraction of coarse mode PM during winter season (Fig. 7).

3.3.2 Summer season

During summer season long range transport from the west and south west contributes significantly to enhanced coarse mode PM mass loadings (Table 2). Long range transport contributes approximately 30 % to coarse mode PM in air masses associated with the south westerly, slow westerly and medium westerly cluster each and 57 % to coarse mode PM in air masses associated with the fast westerly cluster.

Air masses associated with the south easterly cluster (50 $\mu g\,m^{-3}$; Fig. 6) show significantly lower coarse mode PM mass loadings compared to south westerly, slow westerly, medium and fast westerly clusters and also compared to the local air masses observed under calm conditions. Only the difference with respect to the local cluster (80 $\mu g\,m^{-3}$), which represents regional air masses is not significant, mainly due to the high variance of coarse mode PM mass loadings of air masses attributed to the local cluster. The variance is caused by convective dust storms (Joseph, 1982). It is very interesting to note that air masses that have crossed the entire, densely populated IGP show the lowest PM mass loadings even when compared with the local cluster, which represents regional air masses or when compared to air masses representing a local fetch region observed under calm conditions (75 $\mu g\,m^{-3}$). This is true during both rain events and on dry days.

The highest cluster average is observed for the fast westerly cluster (184 $\mu g\,m^{-3}$). The coarse mode PM ($PM_{10-2.5}$) mass loadings for this cluster is significantly enhanced above the coarse mode PM mass loadings observed in all other clusters and under calm conditions (Table 3) and 57 % of the average PM mass is due to long range transport for this cluster. The coarse PM enhancement for the fast westerly cluster is associated with dust storms originating in the Middle East that reach our site from the West (Pandithurai et al., 2008).

The slow and medium westerly cluster and south westerly cluster show enhanced coarse mode PM ($PM_{10-2.5}$) mass loadings as well, though the difference is statistically significant only with respect to the south easterly cluster (Table 2). PM enhancements for the south westerly cluster are associated with dust storms originating from the Thar Desert (Sharma et al., 2012) or the Arabian Peninsula that reach our site through the Indus valley.

During summer season, maximum rainfall is observed for the south-easterly, local cluster, south-westerly and slow westerly cluster in descending order of the absolute rainfall amount. Even when rain events, characterized by average coarse mode PM mass loadings of 50 $\mu g\,m^{-3}$ ($-38\,\%$ in average $PM_{10-2.5}$ mass loading), 29 $\mu g\,m^{-3}$ ($-41\,\%$ in average $PM_{10-2.5}$ mass loading) and 60 $\mu g\,m^{-3}$ ($-50\,\%$ in average $PM_{10-2.5}$ mass loading) for the local, south-easterly and slow westerly cluster respectively and 62 $\mu g\,m^{-3}$ ($-15\,\%$ in average $PM_{10-2.5}$ mass loading) for periods of calm are removed, the differences outlined above remain significant. The south-westerly cluster brings moisture from the Arabian Sea but also dust from the Arabian peninsula (Pease et al., 1998) consequently the average coarse mode PM during rain is comparable to the average coarse mode PM on dry days. It is interesting to note, that the slow westerly cluster shows an increment in fine PM values on rainy days (95 $\mu g\,m^{-3}$) as compared to dry days (84 $\mu g\,m^{-3}$) indicating that rainfall for this cluster is associated with convective dust storms.

For fine mode particulate matter, the slow westerly (84 $\mu g\,m^{-3}$) cluster shows significantly (Table 3) enhanced fine PM mass loadings and approximately 31 % of the fine PM for this cluster is contributed by transport from the west (Table 2). For the slow westerly cluster the differences are significant with respect to the south-easterly cluster (42 $\mu g\,m^{-3}$), south westerly (65 $\mu g\,m^{-3}$), local (58 $\mu g\,m^{-3}$) and medium westerly cluster (60 $\mu g\,m^{-3}$; Fig. 6). Local pollution episodes lead to a 13 % increase above the regional $PM_{2.5}$ background. For the fast westerly cluster (73 $\mu g\,m^{-3}$) 20 % of the fine mode PM is contributed by long range transport but the difference is only significant with respect to the south easterly cluster.

Just like for coarse mode PM, the lowest fine mode PM mass loadings are observed for the south easterly cluster. The difference is significant with respect to the south westerly, slow westerly and fast westerly cluster and with respect to the local pollution episodes observed under calm conditions. (Table 3). Overall fine mode PM mass loadings in summer are lower than during winter time.

During summer season the comparison of the emission ratios of acetonitrile, benzene, CO and NO_2 with fine mode particulate matter pattern indicate that several sources drive fine mode PM (Fig. 8). While there is still a reasonable correlation between CO and $PM_{2.5}$

($r^2 = 0.39$) most other combustion tracers have a poor coefficient of correlation with $PM_{2.5}$. The scatter plots indicate a spread between at least two types of combustion. One type is characterized by high acetonitrile, benzene and NO_2 emissions but fairly low $PM_{2.5}$ mass loadings and is probably associated with wheat residue burning in Punjab, while the other type is characterized by lower benzene, NO_2 and acetonitrile mixing ratios but higher $PM_{2.5}$ mass. This second source is probably traffic, which in arid regions during summer season is responsible for significant (re)-suspension of dust in particular when wind speeds are high ($> 5\,m\,s^{-1}$).

Several authors reported that during summer season, coarse mode mineral dust with a single peak at 3–4 µm optical equivalent diameter dominates PM mass loadings in the IGP (Gautam et al., 2011; Kaskaoutis et al., 2013), however we find that fine mode particulate matter ($PM_{2.5}$) contributes almost equally to PM mass loadings and a significant fraction of $PM_{2.5}$ mass is still combustion derived. Only Jethva et al. (2005), reported a bimodal volume distribution for dust storms with one peak at 3–4 µm and a second peak at 1.5 µm which agrees well with our findings. The peak at 1.5 µm corresponds to the clay fraction of mineral dust and is frequently found to be strongly enriched in mineral dust plumes after extended long-range transport (Pöschl et al., 2010). At our site, we find that the coarse mode PM fraction in individual dust storm events varies between 45 and 92 %, with the highest coarse mode fraction typically recorded for dust storms originating in the Thar Desert. While during dust storms windblown dust contributes significantly to fine mode PM, $PM_{2.5}$ is usually dominated by combustion derived aerosols at our site (Fig. 8).

3.3.3 Monsoon season

During monsoon season the effect of wet scavenging of coarse mode PM mass loadings can be clearly seen in the low average coarse PM mass loadings. Qualitatively the average mass loading is anti-correlated with rainfall. The lowest coarse mode PM mass loadings are observed for the south easterly ($22\,\mu g\,m^{-3}$) and south westerly ($30\,\mu g\,m^{-3}$) cluster.

The slow westerly cluster ($55\,\mu g\,m^{-3}$) shows significant enhancement over all other clusters and the calm periods. Long range transport from the west contributes approximately

30 % to enhanced coarse mode PM mass loadings in the slow westerly cluster (Table 2). However, when rain events are removed, the enhancement over the local cluster is no longer significant.

The local cluster (39 $\mu g\,m^{-3}$) shows enhancements over the south easterly cluster (22 $\mu g\,m^{-3}$) and periods with calm conditions (25 $\mu g\,m^{-3}$), however the enhancement over calm conditions is no longer significant when rain events with average coarse mode PM mass loadings of 22, 25 and 18 $\mu g\,m^{-3}$ respectively are removed from the three clusters (Fig. 6, Table 3).

During monsoon seasons, most coarse mode PM is derived from aqueous phase oxidation of gas phase precursors (Fig. 7), a process that is extremely efficient at RH > 75 % and the removal is controlled by wet scavenging. Dust storms contribute only occasionally to coarse mode PM.

For fine mode PM ($PM_{2.5}$), the south easterly cluster (26 $\mu g\,m^{-3}$) shows the lowest mass loadings. The difference is significant with respect to the local (43 $\mu g\,m^{-3}$) and slow westerly (51 $\mu g\,m^{-3}$) cluster (Fig. 6). The difference between south easterly cluster and calm pollution episodes become significant when only dry days with an average fine PM loading of 26 and 38 $\mu g\,m^{-3}$ respectively are considered (Table 3). The south-westerly cluster (29 $\mu g\,m^{-3}$), too, shows significantly lower fine mode PM when compared to the local (43 $\mu g\,m^{-3}$) and slow westerly (51 $\mu g\,m^{-3}$) cluster (Fig. 6). The slow westerly cluster shows significant enhancements of fine mode PM over all other clusters except the local cluster and significant enhancement over calm periods. Transport contributes approximately 15 % to the fine mode PM for this cluster.

During monsoon season, the correlation of acetonitrile, benzene, CO and NO_2 with fine mode particulate matter indicates that multiple combustion sources drive fine mode PM (Fig. 8). While there is still correlation with CO ($r^2 = 0.44$), the coefficient of correlation of acetonitrile, benzene and NO_2 with $PM_{2.5}$ is low and the largest scatter due to biomass combustion derived $PM_{2.5}$ (associated with high acetonitrile, benzene and NO_2) is observed under calm conditions. $PM_{2.5}$ enhancements for the slow westerly cluster, on the other

hand, are accompanied by low acetonitrile, benzene and NO_2 mixing ratios and are possibly caused by traffic.

3.3.4 Post monsoon season

During post monsoon season air masses reaching the site from the west (slow, medium and fast westerly cluster) show higher coarse PM mass loadings compared to the local cluster and air masses observed under calm conditions. Transport from the west contributes approximately 30 % each to the coarse mode PM mass loadings of the medium westerly and fast westerly cluster and approximately 10 % to the coarse mode PM mass loadings of the slow westerly cluster. The highest coarse mode PM is observed for the fast and medium westerly cluster.

The enhancement in coarse mode PM observed for the medium westerly cluster is statistically significant with respect to all other clusters, including the slow westerly cluster. The enhancement observed for the fast westerly cluster is statistically significant only with respect to the local cluster and calm conditions. Results remain significant even when rain events are removed from both.

Calm episodes have significantly lower coarse mode PM mass loadings (43 $\mu g\,m^{-3}$) than the medium and fast westerly cluster indicating that local pollution episodes are not a significant source of coarse mode PM during post monsoon season, while the fetch region of the westerly clusters are.

The highest fine mode PM during post monsoon season is observed in the fast westerly cluster (97 $\mu g\,m^{-3}$) and transport contributes 18 % to the PM mass loading associated with this cluster (Table 2). Fine PM mass loadings for this cluster are significantly enhanced compared to calm conditions (76 $\mu g\,m^{-3}$) and the local (80 $\mu g\,m^{-3}$) and slow westerly cluster (70 $\mu g\,m^{-3}$). All differences discussed above remain significant when rain events are removed from the dataset and only dry days are considered. The second highest fine mode PM mass loadings are observed for the medium westerly cluster. Transport contributes 11 % to the PM mass loadings observed for this cluster and the source characteristics are similar to those observed for the fast westerly cluster (Fig. 8).

For the slow westerly and local cluster, smoke produced by crop residue burning is a major source of PM during this season as crop residue burning is practised in most of Punjab. Consequently all air masses reaching the receptor site from the West are impacted by this source. Air masses attributed to the slow westerly and local cluster and air masses observed under calm conditions show a clear enhancement in the PM to acetonitrile ratio above the line-fit representing the regional background on days when fresh crop residue burning plumes impact the site. Paddy residue burning leads to massive enhancements in acetonitrile and benzenoids (Sarkar et al., 2013) and equally large emissions of PM. Singh et al. (2010) reported monthly average SPM of 400–500 $\mu g\,m^{-3}$ for a village site near Patiala during October and November and monthly average SPM of 300–400 $\mu g\,m^{-3}$ at a suburban site (residential campus of Punjab University) during the same two months. At our suburban receptor site further downwind of the burning fields we find that PM_{10} generally ranges between 100 and 200 $\mu g\,m^{-3}$ and exceeds 200 $\mu g\,m^{-3}$ only during few episodes. Badrinath et al. (2009) showed that the crop residue burning smoke is mostly channelled into the IGP and Mishra and Shibata (2012) showed that the crop residue burning plumes impact sites as far downwind as Kanpur. During its journey, the smoke ages and aerosol size distributions are modified. Kaskaoutis and co-workers (2013) reported a bi-modal volume size distribution for post monsoon aerosol in Kanpur with a first, peak between 200–300 nm and a second peak at 3–4 µm. In Kanpur, coarse mode aerosol exceeded fine mode PM (by a factor of 1.3), while at our receptor site closer to the burning fields fine mode PM exceeds coarse mode PM by a factor of 1.5. This indicates that during the 720 km journey from Punjab to Kanpur approximately 30 % of the fine particulate matter mass is transformed into coarse mode PM through repeated fog processing.

3.4 Impact of air mass transport on Particulate Matter (PM) exceedance events

The mean PM mass loadings of an air mass cluster represent a poor proxy for the number of BS: ~~days in exceedance of the national air quality standard.~~ exceedance events, that is the number of days on which the 24h average of $PM_{2.5}$ or PM_{10} BS: exceeded the NAAQS of 60 $\mu g\,m^{-3}$ for 24h average $PM_{2.5}$ or 100 $\mu g\,m^{-3}$ for the 24h average PM_{10} respectively. BS: During

winter season on ∼160 days (out of 180 days) the NAAQS of both PM_{10} and $PM_{2.5}$ was exceeded. For summer season, exceedance days associated with PM_{10} were more frequent (203 out of 243 days) that those associated with $PM_{2.5}$ (157 out of 243). During monsoon season, the receptor site received cleaner air masses with only 13 and 21 exceedance days (out of 92) of $PM_{2.5}$ and PM_{10} respectively. Post-monsoon season had frequent exceedance days with NAAQS of PM_{10} and $PM_{2.5}$ being exceeded ∼110 out of 114 days. While individual pollution episodes with extremely high PM mass loadings such as dust storms can profoundly influence the cluster mean, they barely affect the number of exceedance days as such events are rare.

3.4.1 Winter season

During winter season emissions of gas phase precursors and particulate matter from local and regional sources are so high and the conversion of gas phase precursors to both $PM_{2.5}$ and PM_{10} is so efficient, that the NAAQS for both $PM_{2.5}$ and PM_{10} is exceeded 95 % (Fig. 9) of the days associated with the local cluster, i.e. air masses that had been confined over the NW-IGP three days prior to their arrival at the receptor site. Despite the fact that ~~local pollution episodes and~~ transport from the west does enhance PM_{10} mass loadings for the slow, medium and fast westerly cluster, it increased the fraction of days during which PM mass loadings exceed the NAAQS by a maximum of 5 %. ~~both barely increase the fraction of days during which PM mass loadings exceed the NAAQS.~~ The largest increase in the fraction of exceedance days is observed for the south westerly and medium westerly cluster (from 95 to 100 % of the days associated with this synoptic scale transport both for $PM_{2.5}$ and PM_{10}) and the slow westerly cluster (from 95 to ~~91~~ 100 % for PM_{10}). Significantly cleaner air masses with a lower fraction of exceedance events are usually associated with wet scavenging and/or air masses brought by a western disturbance (south-easterly cluster: ~~45~~ 56 % of the days associated with this synoptic scale transport ~~both~~ for $PM_{2.5}$ and 58 % for PM_{10}~~; south-westerly cluster: 45 % of the days associated with this synoptic scale transport for $PM_{2.5}$ and 60 % for PM_{10}).~~ Calm

conditions on the other hand do no increase the percentage of exceedance days for either PM_{10} [BS:] or $PM_{2.5}$ [BS:] when compared to the local cluster.

3.4.2 Summer season

[BS:] As discussed in section 3.3.2, during summer season,[BS:] the ambient RH is usually <60 % at night and 20-30 % during the day (Table 1) and aqueous phase oxidation contributes less to $PM_{2.5}$ and PM_{10} mass loadings. Instead, PM mass is dominated by direct emissions, dust and photochemistry.

Despite frequent dust storms, exceedance events are less frequent during summer season than they are during winter season. The NAAQS for PM_{10} is exceeded [BS:] ~~6~~[BS:] 80 % of the days associated with the local cluster and the NAAQS for $PM_{2.5}$ is exceeded [BS:] ~~4~~[BS:] 70 % of the days associated with this synoptic scale transport. While dust storms – episodic events during which PM_{10} mass loadings can reach up to 3000 $\mu g\,m^{-3}$ – have a strong impact on the cluster mean in particular for the fast westerly cluster; they barely affect the number of exceedance events. This is particularly true for the fast and medium westerly cluster. Only for the south westerly cluster, dust storms increase the number of exceedance events compared to the local cluster from [BS:] ~~6~~[BS:] 80 to [BS:] ~~8~~[BS:] 100 % of the days associated with this synoptic scale transport for PM_{10}. The highest increase in the number of exceedance events for $PM_{2.5}$ is observed for the slow westerly cluster, which is most strongly affected by wheat residue burning in Punjab. Wheat residue burning increases the number of exceedance events observed for the slow westerly cluster compared to the local cluster [BS:] ~~by 4~~[BS:] 70 to [BS:] ~~7~~[BS:] 80 % of the days associated with this synoptic scale transport for $PM_{2.5}$ and from [BS:] ~~6~~[BS:] 80 to [BS:] ~~80~~[BS:] 95 % for PM_{10}. The fraction of exceedance events for the south-easterly cluster, both for PM_{10} and $PM_{2.5}$ ([BS:] ~~34~~[BS:] 50 % and [BS:] ~~20~~[BS:] 30 % of the days with this synoptic scale transport, respectively) is associated with cleaner air masses reaching the receptor site from the eastern IGP.[BS:] Calm conditions barely increase the number of exceedance days.

3.4.3 Monsoon season

[BS:] During monsoon season the number of exceedance events is controlled by the interplay of wet scavenging emissions and aqueous phase oxidation of gas phase precursors.

Fig. 9 [BS:] shows that the frequency of $PM_{2.5}$ exceedance days for each cluster is anti-correlated with the total rainfall observed for the respective [BS:] For the local cluster, the NAAQS for PM_{10} [BS:] is exceeded 48 % [BS:] of the days and the NAAQS for $PM_{2.5}$ [BS:] is exceeded 36 % [BS:] of the days associated with this synoptic scale transport. The slow westerly cluster which is associated with occasional dust storms increases the percentage of exceedance days from 36 % [BS:] to 60 % [BS:] for $PM_{2.5}$ [BS:] and from 48 % [BS:] to 80 % [BS:] for PM_{10} [BS:]. The fraction of exceedance events for the south-easterly cluster, both for PM_{10} [BS:] (6 % [BS:] of the days associated with this synoptic scale transport) and $PM_{2.5}$ [BS:] (0 % [BS:] of the days associated with this synoptic scale transport) is associated with extremely clean air masses reaching the receptor site from the eastern IGP. cluster. [BS:] For PM_{10} [BS:] the high number of PM_{10} [BS:] exceedance events for the local cluster stands out. The local cluster shows a higher degree of cloudiness compared to the slow westerly cluster (indicated by the lower average daytime solar radiation, Table 2 [BS:]) and slightly less cloudiness compared to calm conditions. The number of rain events and the total amount of rainfall for the local cluster is higher compared to the rainfall and number of rain events observed for the slow westerly cluster. Under calm conditions, on the other hand, drizzle occurs very frequently. PM_{10} [BS:] exceedance events seem to correlate with the number of precipitation-free cloud-cycles through which the aerosol is processed. Despite the fact that the number of rain events and the total amount of rainfall is higher for the local cluster and despite the fact that dust storms occasionally contribute to coarse mode PM mass loadings for the slow westerly cluster, the number of PM_{10} [BS:] exceedance events for the local cluster is higher than the number of PM_{10} [BS:] exceedance events for the slow westerly cluster.

3.4.4 Post monsoon season

[BS:] During post-monsoon season crop residue burning coupled with aqueous phase oxidation of gas phase precursors again leads to a high frequency of exceedance events. [BS:] As discussed in sec-

tion 3.3.4, crop residue burning coupled with aqueous phase oxidation of gas phase precursors is responsible for high PM mass loading during post-monsoon season. It can be seen from Fig. 9 BS: that it also contributes to a high frequency of exceedance events. The NAAQS for both $PM_{2.5}$ and PM_{10} is exceeded BS: 65 and 70–75 BS: 90–100 % of the days associated with the synoptic scale transport for the local BS: , BS: and slow westerly BS: , medium westerly, fast westerly cluster and under calm conditions. Transport BS: barely leads to an increase in the fraction of exceedance days BS: . BS: to 73 and 94 % BS: of the days associated with the synoptic scale transport for $PM_{2.5}$ BS: both for the medium and fast westerly cluster respectively and to an increase in the fraction of exceedance days to 91 and 94 % BS: of the days associated with the synoptic scale transport for the medium and fast westerly cluster respectively for PM_{10} BS: .

4 Conclusions

We investigated the contribution of long range transport and local pollution episodes to the average coarse and fine mode PM mass loadings at our receptor site using two years of high temporal resolution data. BS: The study yielded several results as follows:

1. Long range transport from the west BS: (Source region: Arabia, Thar desert, Middle East and Afghanistan) leads to significant enhancements in the average coarse mode PM mass loadings during all seasons. BS: The contribution of long range transport from this source region to coarse mode PM varied between 9 % to 57 % BS: of the total $PM_{10-2.5}$ BS: mass.

   BS: For the slow westerly cluster the contribution of long range transport to coarse mode PM varies between 9 % BS: during post monsoon season and 34 % BS: during summer season. For the medium westerly cluster the contribution of transport to coarse mode PM is 30 % BS: during all seasons and for the fast westerly cluster the contribution of long range transport to coarse PM mass loadings varies between 18 and 57 %. BS: For the south westerly cluster transport leads to enhanced coarse mode PM only during winter (9 %) and summer (34 %) BS: season.

~~During monsoon season PM mass loadings for this cluster are significantly lower compared to the local cluster thanks to the effect of wet scavenging.~~

2. [BS:] For fine mode PM the situation is more complex. The fast westerly cluster is associated with a 20 % [BS:] increase in fine mode PM during summer and post monsoon season but cleaner air masses during winter season. The medium westerly cluster shows moderately enhanced PM mass loadings during all seasons while slow westerly transport leads to enhanced $PM_{2.5}$ [BS:] mass loadings during winter, summer and monsoon season but not during post monsoon season.

3. Local pollution episodes [BS:] (wind speed $< 1\,m\,s^{-1}$) [BS:] contributed to enhanced $PM_{2.5}$ [BS:] mass loadings during both winter and summer season and to enhanced coarse mode PM only during winter season.

4. The south easterly cluster [BS:] (Source region: Eastern IGP) is associated with significantly lower fine and coarse mode PM mass loadings during all seasons.

   ~~[BS:] For fine mode PM the situation is more complex. The fast westerly cluster is associated with a 20 % [BS:] increase in fine mode PM during summer and post monsoon season but cleaner air masses during winter season. The medium westerly cluster shows moderately enhance PM mass loadings during all seasons while slow westerly transport leads to enhanced $PM_{2.5}$ [BS:] mass loadings during winter, summer and monsoon season but not during post monsoon season. The south easterly cluster is associated with significantly lower $PM_{2.5}$ [BS:] mass loadings during all seasons.~~

5. The number of days during which PM mass loadings exceed the national ambient air quality standard (NAAQS) of $100\,\mu g\,m^{-3}$ for 24 h average PM_{10} and $60\,\mu g\,m^{-3}$ for 24 h average $PM_{2.5}$ (NAAQS, 2009), however is controlled by long range transport to a much lesser degree.

   For the local cluster, which represents regional air masses (Source region: NW-IGP), the fraction of days during which the national ambient air quality standard (NAAQS) of $60\,\mu g\,m^{-3}$ for 24 h average $PM_{2.5}$ was exceeded varied between [BS:] ~~22~~ [BS:] 36 % [BS:] ~~of the~~

days associated with this synoptic scale transport during monsoon season and [BS:] 85 [BS:] 95 % of the days associated with this synoptic scale transport during [BS:] monsoon season and winter [BS:] and post monsoon season [BS:] respectively; the fraction of days during which the national ambient air quality standard (NAAQS) of 100 $\mu g\,m^{-3}$ for the 24 h average PM_{10} was exceeded, varied between [BS:] 37 [BS:] 48 % during monsoon season and [BS:] 84 [BS:] 98 % during [BS:] winter [BS:] post monsoon season.

6. Long range transport was responsible for both bringing air masses with a significantly lower fraction of exceedance days from the Eastern IGP and air masses with a moderate increase in the fraction of exceedance days from the West (Source region: Arabia, Thar desert, Middle East and Afghanistan). The south easterly cluster (Source region: Eastern IGP) is always associated with a significantly lower fraction of exceedance days and the south westerly cluster also leads to a lower fraction of exceedance days during [BS:] winter and monsoon season.

   Whenever long range transport increases the fraction of exceedance days the increase varies between a few percent and at most [BS:] 3 [BS:] 20 %.

   [BS:] In order to bring PM mass loadings in compliance with the national ambient air quality standard (NAAQS) and reduce the number of exceedance days, mitigation of regional pollution sources needs to be given highest priority as the number of exceedance days for air masses associated with the source region NW-IGP is already extremely high.

7. Fine mode PM ($PM_{2.5}$) contributes most to PM exceedance events at a regional level and $PM_{2.5}$ mass loadings are largely controlled by combustion sources during all seasons. Primary emission and gas to particle conversion of gas phase precursors emitted during the combustion, both contribute to the final mass loadings in varying proportions.

   [BS:] In order to bring PM mass loadings in compliance with the national ambient air quality standard (NAAQS) and reduce the number of exceedance days, mitigation of regional [BS:] pollution combustion [BS:] sources needs to be given highest priority as the

number of exceedance days for air masses associated with the source region NW-IGP is already extremely high.

To devise efficient mitigation strategies targeted at bringing down the number of PM exceedance events, a larger set of tracers needs to be incorporated and alternate source receptor modelling approaches e.g. PMF modelling targeted specifically towards identifying local and regional combustion sources contributing towards the emissions of PM and towards the emission gas phase aerosol precursors need to be adopted.

The Supplement related to this article is available online at doi:10.5194/acpd-0-1-2015-supplement.

Acknowledgements. We thank the IISER Mohali Atmospheric Chemistry Facility for data and the Ministry of Human Resource Development (MHRD), India and IISER Mohali for funding the facility.

We thank the NOAA Air Resources Laboratory (ARL) for the provision of the HYSPLIT transport and dispersion model used in this study. We thank the ESA GlobCover 2009 Project (ESA 2010 and UCLouvain) for providing a high resolution land classification map of the region.

Harshita Pawar, Himanshu Sachan and Vinod Kumar gratefully acknowledge a DST Inspire fellowship, Boggarapu Prafulla Chandra acknowledges CSIR-JRF fellowship and Ruhani Arya gratefully acknowledges the IISER Mohali summer research fellowship program. Boggarapu Praphulla Chandra, Chinmoy Sarkar and Saryu Garg acknowledge a 6 month project assistant position funded by the DST – Max Planck Research Partner Group on “Tropospheric OH reactivity and VOC measurements”.

References

Abdalmogith, S. S., and Harrison, R. M.: The use of trajectory cluster analysis to examine the long-range transport of secondary inorganic aerosol in the UK, Atmos. Environ., 39, 6686–6695, doi:10.1016/j.atmosenv.2005.07.059, 2005.

Agnihotri, C. and Singh, M.: Satellite study of western disturbances, Mausam, 33, 249–254, 1982.
Akagi, S. K., Yokelson, R. J., Wiedinmyer, C., Alvarado, M. J., Reid, J. S., Karl, T., Crounse, J. D., and Wennberg, P. O.: Emission factors for open and domestic biomass burning for use in atmospheric models, Atmos. Chem. Phys., 11, 4039–4072, doi:10.5194/acp-11-4039-2011, 2011.
Badarinath, K., Kharol, S. K., Sharma, A. R., and Krishna Prasad, V.: Analysis of aerosol and carbon monoxide characteristics over Arabian Sea during crop residue burning period in the Indo-Gangetic Plains using multi-satellite remote sensing datasets, J. Atmos. Sol.-Terr. Phy., 71, 1267–1276, 2009.
Bell, M. L. and Davis, D. L.: Reassessment of the lethal London fog of 1952: novel indicators of acute and chronic consequences of acute exposure to air pollution, Environ. Health Persp., 109, 389–394, 2001.
Bhat, G. S.: The Indian drought of 2002 a sub-seasonal phenomenon?, Q. J. Roy. Meteor. Soc., 132, 2583–2602, doi:10.1256/qj.05.13, 2006.
Borge, R., Lumbreras, J., Vardoulakis, S., Kassomenos, P., and Rodríguez, E.: Analysis of long-range transport influences on urban PM_{10} using two-stage atmospheric trajectory clusters, Atmos. Environ., 41, 4434–4450, doi:10.1016/j.atmosenv.2007.01.053, 2007.
Bow, S.-T.: Pattern Recognition: Application to Large Data-Set Problems, Marcel Dekker Inc., New York, 1984.
Brankov, E., Rao, S. T., and Porter, P. S.: A trajectory-clustering-correlation methodology for examining the long-range transport of air pollutants, Atmos. Environ., 32, 1525–1534, doi:10.1016/S1352-2310(97)00388-9, 1998.
Bryson, R. A. and Swain, A. M.: Holocene variations of monsoon rainfall in Rajasthan, Quaternary Res., 16, 135–145, doi:10.1016/0033-5894(81)90041-7, 1981.
Buchanan, C. M., Beverland, I. J., and Heal, M. R.: The influence of weather-type and longrange transport on air particle concentrations in Edinburgh, U K., Atmos. Environ., 36, 5343–5354, 2002.
Das, P. K.: Mean vertical motion and non-adiabatic heat sources over India during the monsoon, Tellus, 14, 212–220, doi:10.1111/j.2153-3490.1962.tb00132.x, 1962.
Dey, S., and Tripathi, S.: Estimation of aerosol optical properties and radiative effects in the Ganga basin, northern India, during the wintertime, J. Geophys. Res.-Atmos., 112, D03203, doi:10.1029/2006jd007267, 2007.
Dimri, A. P.: Impact of horizontal model resolution and orography on the simulation of a western disturbance and its associated precipitation, Meteorol. Appl., 11, 115–127, doi:10.1017/S1350482704001227, 2004.

Dockery, D. W., Speizer, F. E., Stram, D. O., Ware, J. H., Spengler, J. D., and Ferris Jr., B. G.: Effects of inhalable particles on respiratory health of children, Am. Rev. Respir. Dis., 139, 587–594, 1989.

Dockery, D. W., Pope, C. A., Xu, X., Spengler, J. D., Ware, J. H., Fay, M. E., Ferris Jr, B. G., and Speizer, F. E.: An association between air pollution and mortality in six US cities, New Engl. J. Med., 329, 1753–1759, 1993.

Dorling, S. R., Davies, T. D., and Pierce, C. E.: Cluster analysis: a technique for estimating the synoptic meteorological controls on air and precipitation chemistry – Method and applications, Atmos. Environ. A-Gen., 26, 2575–2581, doi:10.1016/0960-1686(92)90110-7, 1992.

Draxler, R. and Rolph, G.: HYSPLIT (HYbrid Single-Particle Lagrangian Integrated Trajectory) NOAA Air Resources Laboratory, College Park, MD, Model access via NOAA ARL READY Website, 2013.

Draxler, R. R. and Hess, G.: An overview of the HYSPLIT_4 modelling system for trajectories, Aust. Meteorol. Mag., 47, 295–308, 1998.

Englert, N.: Fine particles and human health – a review of epidemiological studies, Toxicol. Lett., 149, 235–242, 2004.

Firket, J.: The cause of the symptoms found in the Meuse Valley during the fog of December, 1930, Bull. Acad. R. Med. Belg., 11, 683–741, 1931.

Fleming, Z. L., Monks, P. S., and Manning, A. J.: Review: Untangling the influence of air-mass history in interpreting observed atmospheric composition, Atmos. Res., 104–105, 1–39, doi:10.1016/j.atmosres.2011.09.009, 2012.

Gautam, R., Hsu, N. C., Tsay, S. C., Lau, K. M., Holben, B., Bell, S., Smirnov, A., Li, C., Hansell, R., Ji, Q., Payra, S., Aryal, D., Kayastha, R., and Kim, K. M.: Accumulation of aerosols over the Indo-Gangetic plains and southern slopes of the Himalayas: distribution, properties and radiative effects during the 2009 pre-monsoon season, Atmos. Chem. Phys., 11, 12841–12863, doi:10.5194/acp-11-12841-2011, 2011.

Goswami, B. N.: Interannual variations of indian summer monsoon in a GCM: external conditions versus internal feedbacks, J. Climate, 11, 501–522, doi:10.1175/1520-0442(1998)011<0501:IVOISM>2.0.CO;2, 1998.

Goswami, B. N., Venugopal, V., Sengupta, D., Madhusoodanan, M. S., and Xavier, P. K.: Increasing trend of extreme rain events over india in a warming environment, Science, 314, 1442–1445, doi:10.1126/science.1132027, 2006a.

Goswami, B. N., Wu, G., and Yasunari, T.: The annual cycle, intraseasonal oscillations, and roadblock to seasonal predictability of the asian summer monsoon, J. Climate, 19, 5078–5099, doi:10.1175/JCLI3901.1, 2006b.

Grivas, G., Chaloulakou, A., and Kassomenos, P.: An overview of the PM_{10} pollution problem, in the Metropolitan Area of Athens, Greece, assessment of controlling factors and potential impact of long range transport, Sci. Total Environ., 389, 165–177, doi:10.1016/j.scitotenv.2007.08.048, 2008.

Habib, G., Venkataraman, C., Shrivastava, M., Banerjee, R., Stehr, J., and Dickerson, R. R.: New methodology for estimating biofuel consumption for cooking: atmospheric emissions of black carbon and sulfur dioxide from India, Global Biogeochem. Cy., 18, GB3007, doi:10.1029/2003gb002157, 2004.

Jethva, H., Satheesh, S. K., and Srinivasan, J.: Seasonal variability of aerosols over the Indo-Gangetic basin, J. Geophys. Res., 110, D21204, doi:10.1029/2005JD005938, 2005.

Joseph, P.: A tentative model of Andhi, Mausam, 33, 417–422, 1982.

Joseph, P. and Raman, P.: Existence of low level westerly jet stream over peninsular India during July, Indian J. Meteorol. Geophys., 17, 407–410, 1966.

Joseph, P. V. and Sijikumar, S.: Intraseasonal Variability of the Low-Level Jet Stream of the Asian Summer Monsoon, J. Climate, 17, 1449–1458, doi:10.1175/1520-0442(2004)017<1449:IVOTLJ>2.0.CO;2, 2004.

Kappos, A. D., Bruckmann, P., Eikmann, T., Englert, N., Heinrich, U., Höppe, P., Koch, E., Krause, G. H., Kreyling, W. G., and Rauchfuss, K.: Health effects of particles in ambient air, Int. J. Hyg. Envir. Heal., 207, 399–407, 2004.

Kaskaoutis, D., Sinha, P., Vinoj, V., Kosmopoulos, P., Tripathi, S., Misra, A., Sharma, M., and Singh, R.: Aerosol properties and radiative forcing over Kanpur during severe aerosol loading conditions, Atmos. Environ., 79, 7–19, 2013.

Kassomenos, P., Vardoulakis, S., Borge, R., Lumbreras, J., Papaloukas, C., and Karakitsios, S.: Comparison of statistical clustering techniques for the classification of modelled atmospheric trajectories, Theor. Appl. Climatol., 102, 1–12, doi:10.1007/s00704-009-0233-7, 2010.

Kaushik, C., Ravindra, K., Yadav, K., Mehta, S., and Haritash, A.: Assessment of ambient air quality in urban centres of Haryana (India) in relation to different anthropogenic activities and health risks, Environ. Monit. Assess., 122, 27–40, 2006.

Kulshrestha, U. C., Saxena, A., Kumar, N., Kumari, K. M., and Srivastava, S. S.: Chemical composition and association of size-differentiated aerosols at a suburban site in a semi-arid tract of India, J. Atmos. Chem., 29, 109–118, doi:10.1023/A:1005796400044, 1998.
Kumar, R., Srivastava, S., and Kumari, K. M.: Characteristics of aerosols over suburban and urban site of semiarid region in India: seasonal and spatial variations, Aerosol Air Qual. Res., 7, 531–549, 2007.
Lang, T. J., and Barros, A. P.: Winter storms in the Central Himalayas, J. Meteorol. Soc. Jpn., 82, 829–844, doi:10.2151/jmsj.2004.829, 2004.
Lawrence,M. G., and Lelieveld, J.: Atmospheric pollutant outflow from southern Asia: a review, Atmos. Chem. Phys., 10, 11017–11096, doi:10.5194/acp-10-11017-2010, 2010.
Logan, W.: Mortality in the London fog incident, 1952, Lancet, 261, 336–338, 1953.
Massey, D., Masih, J., Kulshrestha, A., Habil, M., and Taneja, A.: Indoor/outdoor relationship of fine particles less than 2.5 µm ($PM_{2.5}$) in residential homes locations in central Indian region, Build. Environ., 44, 2037–2045, 2009.
Miller, L., Farhana, S., and Xu, X.: Trans-boundary air pollution in Windsor, Ontario (Canada), Procedia Environmental Sciences, 2, 585–594, doi:10.1016/j.proenv.2010.10.064, 2010.
Mishra, A. K. and Shibata, T.: Synergistic analyses of optical and microphysical properties of agricultural crop residue burning aerosols over the Indo-Gangetic Basin (IGB), Atmos. Environ., 57, 205–218, 2012.
Mohanraj, R. and Azeez, P.: Health effects of airborne particulate matter and the Indian scenario, Curr. Sci. India, 87, 741–748, 2004.
Mooley, D.: The role of western disturbances in the production of weather over India during different seasons, Indian J. Meteor. Geophys., 8, 253–260, 1957.
NAAQS: National Ambient Air Quality Standard 2009, The Gazette of India, Extraordinary, Kartika 27, 1931, Government of India, New Delhi, 2009.
Nag, S., Gupta, A., and Mukhopadhyay, U.: Size distribution of atmospheric aerosols in Kolkata, India and the assessment of pulmonary deposition of particle mass, Indoor Built Environ., 14, 381–389, 2005.
Nemery, B., Hoet, P. H., and Nemmar, A.: The Meuse Valley fog of 1930: an air pollution disaster, Lancet, 357, 704–708, 2001.
Nyanganyura, D., Makarau, A., Mathuthu, M., and Meixner, F. X.: A five-day back trajectory climatology for Rukomechi research station (northern Zimbabwe) and the impact of large-scale atmo-

spheric flows on concentrations of airborne coarse and fine particulate mass, S. Afr. J. Sci., 104, 43–52, 2008.
Pandey, J. S., Kumar, R., and Devotta, S.: Health risks of NO_2, SPM and SO_2 in Delhi (India), Atmos. Environ., 39, 6868–6874, 2005.
Pandithurai, G., Dipu, S., Dani, K., Tiwari, S., Bisht, D., Devara, P., and Pinker, R.: Aerosol radiative forcing during dust events over New Delhi, India, J. Geophys. Res.-Atmos., 113, D13209, doi:10.1029/2008jd009804, 2008.
Pease, P. P., Tchakerian, V. P., and Tindale, N. W.: Aerosols over the Arabian Sea: geochemistry and source areas for aeolian desert dust, J. Arid Environ., 39, 477–496, 1998.
Pisharoty, P. and Desai, B.: Western disturbances and Indian weather, Indian J. Meteorol. Geophys., 8, 333–338, 1956.
Pope III, C.: Epidemiology of fine particulate air pollution and human health: biologic mechanisms and who's at risk?, Environ. Health Persp., 108, 713–723, 2000.
Pope III, C. A., Thun, M. J., Namboodiri, M. M., Dockery, D. W., Evans, J. S., Speizer, F. E., and Heath Jr, C. W.: Particulate air pollution as a predictor of mortality in a prospective study of US adults, Am. J. Resp. Crit. Care, 151, 669–674, 1995.
Pope III, C. A., and Dockery, D. W.: Health effects of fine particulate air pollution: lines that connect, J. Air Waste Manage., 56, 709–742, 2006.
Pöschl, U., Martin, S. T., Sinha, B., Chen, Q., Gunthe, S. S., Huffman, J. A., Borrmann, S., Farmer, D. K., Garland, R. M., Helas, G., Jimenez, J. L., King, S. M., Manzi, A., Mikhailov, E., Pauliquevis, T., Petters, M. D., Prenni, A. J., Roldin, P., Rose, D., Schneider, J., Su, H., Zorn, S. R., Artaxo, P., and Andreae, M. O.: Rainforest aerosols as biogenic nuclei of clouds and precipitation in the Amazon, Science, 329, 1513–1516, doi:10.1126/science.1191056, 2010.
Ramaswamy, C.: On the sub-tropical jet stream and its role in the development of large-scale convection, Tellus, 8, 26–60, 1956.
Rao, P. S. and Sikka, D. R.: Intraseasonal variability of the summer monsoon over the North Indian Ocean as revealed by the BOBMEX and ARMEX field programs, Pure Appl. Geophys., 162, 1481–1510, doi:10.1007/s00024-005-2680-0, 2005.
Sarkar, C., Kumar, V., and Sinha, V.: Massive emissions of carcinogenic benzenoids from paddy residue burning in North India, Curr. Sci. India, 104, 1703–1706, 2013.
Schrenk, H. H., Heimann, H., Clayton, G. D., Gafafer, W., and Wexler, H.: Air Pollution in Donora, Pa. Epidemiology of the Unusual Smog Episode of October 1948, Preliminary Report, Public Health

Bulletin, no 306, Washington, D.C. : Federal Security Agency, Public Health Service, Bureau of State Services, Division of Industrial Hygiene, 173 pp., 1949.
Schwartz, J.: Air pollution and daily mortality: a review and meta analysis, Environ. Res., 64, 36–52, 1994.
Sharma, D., Singh, D., and Kaskaoutis, D.: Impact of two intense dust storms on aerosol characteristics and radiative forcing over Patiala, northwestern India, Advances in Meteorology, 2012, 956814, doi:10.1155/2012/956814, 2012.
Shy, C. M.: Epidemiologic evidence and the United States air quality standards, Am. J. Epidemiol., 110, 661–671, 1979.
Sikka, D.: Evaluation of monitoring and forecasting of summer monsoon over India and a review of monsoon drought of 2002, Proceedings – Indian National Science Academy Part A, 69, 479–504, 2003.
Sikka, D. R. and Gadgil, S.: On the maximum cloud zone and the ITCZ over Indian, longitudes during the Southwest Monsoon, Mon. Weather Rev., 108, 1840–1853, doi:10.1175/1520-0493(1980)108<1840:OTMCZA>2.0.CO;2, 1980.
Singh, N., Mittal, S. K., Agarwal, R., Awasthi, A., and Gupta, P. K.: Impact of rice crop residue burning on levels of SPM, SO_2 and NO_2 in the ambient air of Patiala (India), Int. J. Environ. An. Ch., 90, 829–843, 2010.
Sinha, V., Kumar, V., and Sarkar, C.: Chemical composition of pre-monsoon air in the Indo-Gangetic Plain measured using a new air quality facility and PTR-MS: high surface ozone and strong influence of biomass burning, Atmos. Chem. Phys., 14, 5921–5941, doi:10.5194/acp-14-5921-2014, 2014.
Stohl, A.: Trajectory statistics – a new method to establish source-receptor relationships of air pollutants and its application to the transport of particulate sulfate in Europe, Atmos. Environ., 30, 579–587, doi:10.1016/1352-2310(95)00314-2, 1996.
Stohl, A.: Computation, accuracy and applications of trajectories – a review and bibliography, Atmos. Environ., 32, 947–966, doi:10.1016/S1352-2310(97)00457-3, 1998.
Venkataraman, C., Habib, G., Eiguren-Fernandez, A., Miguel, A., and Friedlander, S.: Residential biofuels in South Asia: carbonaceous aerosol emissions and climate impacts, Science, 307, 1454–1456, 2005.
Ware, J. H., Thibodeau, L. A., Speizer, F. E., Colóme, S., and Ferris Jr, B. G.: Assessment of the health effects of atmospheric sulfur oxides and particulate matter: evidence from observational studies, Environ. Health Persp., 41, 255–276, 1981.

Table 1. Average of the locally measured meteorological parameters for daytime/nighttime for the different clusters and seasons.For solar radiation we provided the daytime average only. For rain we calculated the sum of the rainfall instead of the average and the numbers in brackets represent the number of rain events.

	Fast Westerly	Medium Westerly	Slow Westerly	Local	South Westerly	South Easterly	Calm
				WINTER (Dec–Feb)			
T (°C)	18.9/8.5	17.7/9.4	17.5 / 9.3	17.7/9.8	15.6/12.7	18.3/12.0	16.6/10.4
RH (%)	43.6/82.5	49.5/79.6	50.0/79.5	53.7/79.9	57.8/74.5	57.2/77.8	62.2/79.7
Wind Speed ($m\,s^{-1}$)	7.0/5.0	8.2/3.2	5.7/3.0	5.4/3.5	5.4/6.0	6.9/4.8	0.8/0.7
Wind Direction	302/319	270/303	306/294	292/304	298/240	241/188	235/139
Absolute Humidity ($g\,m^{-3}$)	7.4 /7.2	7.9/7.3	7.8/7.3	8.5/7.6	8.1/8.6	9.4/8.5	9.2/7.9
Solar Radiation ($W\,m^{-2}$)	414	331	381	376	362	338	307
Rain (mm)	–	–	–	7.7 (2)	–	50.7 (11)	27.3 (8)
				SUMMER (Mar–Jun)			
T (°C)	31.7/19.3	32.6/20.3	35.9/26.5	32.1/22.7	32.5/25.2	29.5/22.9	34.2/23.3
RH (%)	23.4/58.8	22.1/50.7	24.3/44.7	28.7/51.8	36.2/52.5	44.1/64.1	29.0/53.3
Wind Speed ($m\,s^{-1}$)	9.1/5.6	7.6/3.6	7.7/4.5	7.2/4.3	7.9/4.5	7.0/5.6	0.9/0.7
Wind Direction	312/308	306/124	288/280	298/264	182/135	171/152	209/186
Absolute Humidity ($g\,m^{-3}$)	8.1/10.3	8.0/9.4	10.3 /11.7	10.0/11.0	12.9/12.8	13.5/13.8	11.3/11.7
Solar Radiation ($W\,m^{-2}$)	633	607	593	586	519	569	548
Rain (mm)	–	–	8.5 (3)	28.5 (5)	18.6 (2)	35.8 (10)	27 (27)
				MONSOON (Jul–Sep)			
T (°C)	–	–	32.9/25.6	32.4/26.3	30.6/26.0	31.3/27.1	32.3/26.5
RH (%)	–	–	50.5/80.1	57.5/82.0	68.0/85.2	64.9/81.8	61.7/83.6
Wind Speed ($m\,s^{-1}$)	–	–	8.5/4.5	6.4/3.2	5.4/4.1	6.3/4.2	0.8/0.7
Wind Direction	–	–	309/191	280/148	182/124	166/128	206/132
Absolute Humidity ($g\,m^{-3}$)	–	–	18.4/19.9	20.4/21.2	22.0/21.7	21.7/22.1	21.8/21.8
Solar Radiation ($W\,m^{-2}$)	–	–	565	515	430	472	499
Rain (mm)	–	–	0.4(1)	33.8(4)	74.1(3)	142.2 (9)	36 (29)
				POST-MONSOON (Oct–Nov)			
T (°C)	23.3/12.8	23.6/12.9	28.0/18.2	27.3/17.3	–	–	28.1/17.4
RH (%)	35.7/72.9	22.3/74.2	34.1/64.2	34.9/67.7	–	–	34.6/68.0
Wind Speed ($m\,s^{-1}$)	6.3/2.9	9.2/3.9	5.5/2.7	5.3/2.6	–	–	0.7/0.7
Wind Direction	310/175	313/315	310/71	304/174	–	–	214/115
Absolute Humidity ($g\,m^{-3}$)	7.7/8.5	8.0/8.7	9.7/10.5	9.5/10.4	–	–	9.8/10.6
Solar Radiation ($W\,m^{-2}$)	409	417	447	422	–	–	461
Rain (mm)	–	–	–	3.1 (2)	–	–	0.8 (2)

Table 2. Lower limit for the contribution of long range transport and local pollution events to PM mass loadings in % $^{BS:}\pm 1\sigma$ of the total PM. "Negative" indicates that the PM mass loadings are not enhanced compared to the local cluster, which represent the regional background levels.

	Fast Westerly	Medium Westerly	Slow Westerly	South Westerly	South Easterly	Calm
			$PM_{2.5}$			
Winter	Negative	7 $^{BS:}\pm 4$	13 $^{BS:}\pm 9$	Negative	Negative	22 $^{BS:}\pm 15$
Summer	20 $^{BS:}\pm 15$	4 $^{BS:}\pm 3$	31 $^{BS:}\pm 21$	10 $^{BS:}\pm 8$	Negative	13 $^{BS:}\pm 8$
Monsoon	Negative	Negative	15 $^{BS:}\pm 11$	Negative	Negative	Negative
Post-Monsoon	18 $^{BS:}\pm 10$	11 $^{BS:}\pm 7$	Negative	Negative	Negative	Negative
			$PM_{10-2.5}$			
Winter	18 $^{BS:}\pm 8$	28 $^{BS:}\pm 16$	22 $^{BS:}\pm 15$	9 $^{BS:}\pm 5$	Negative	$^{BS:}14 \pm 10$
Summer	57 $^{BS:}\pm 49$	27 $^{BS:}\pm 21$	34 $^{BS:}\pm 28$	34 $^{BS:}\pm 26$	Negative	Negative
Monsoon	Negative	Negative	29 $^{BS:}\pm 11$	Negative	Negative	Negative
Post-Monsoon	27 $^{BS:}\pm 18$	31 $^{BS:}\pm 21$	9 $^{BS:}\pm 6$	Negative	Negative	Negative

Table 3. Statistical significance of the difference of the mean for each pair of clusters.Values to the right of the principal diagonal denote significance among $PM_{10-2.5}$ pairs while values to the left of the principal diagonal denote significance among $PM_{2.5}$ pairs. Pair wise comparison based on Tukey's studentised HSD test (Honestly significant differences) test was used to assess the statistical significance of the difference of the mean for each pair of clusters and each season. Values in brackets indicate the statistical significance after all rain events were removed from the dataset.

	Calm	South Easterly	South Westerly	Local	Slow Westerly	Medium Westerly	Fast Westerly
WINTER (Dec–Feb)							
Calm	–						
South Easterly	3σ (3σ)	–					
South Westerly	1σ(1σ)		–				
Local	– (1σ)	1σ		–			
Slow Westerly		2σ (1σ)			–		
Medium Westerly		1σ				–	
Fast Westerly	1σ (1σ)						–
SUMMER (Mar–Jun)							
Calm	–						4σ (3σ)
South Easterly	2σ (2σ)	–	2σ (1σ)		2σ (1σ)	1σ (1σ)	4σ (4σ)
South Westerly		1σ (1σ)	–				1σ (1σ)
Local				–			4σ (3σ)
Slow Westerly		4σ (4σ)	1σ (1σ)	2σ (2σ)	–		1σ (1σ)
Medium Westerly		1σ			1σ (1σ)	–	2σ (2σ)
Fast Westerly		2σ (2σ)					–
MONSOON (Jul–Sep)							
Calm	–			1σ	3σ (2σ)		
South Easterly	– (1σ)	–		1σ (1σ)	4σ (3σ)		
South Westerly			–		2σ (1σ)		
Local		2σ (2σ)	2σ (1σ)	–	1σ		
Slow Westerly	2σ (1σ)	4σ (4σ)	3σ (2σ)		–		
Medium Westerly						–	
Fast Westerly							–
POST-MONSOON (Oct–Nov)							
Calm	–					3σ (3σ)	2σ (2σ)
South Easterly		–					
South Westerly			–				
Local				–		2σ (1σ)	1σ (1σ)
Slow Westerly					–	1σ (1σ)	
Medium Westerly					1σ (1σ)	–	
Fast Westerly	1σ (1σ)			1σ (1σ)	2σ (2σ)		–

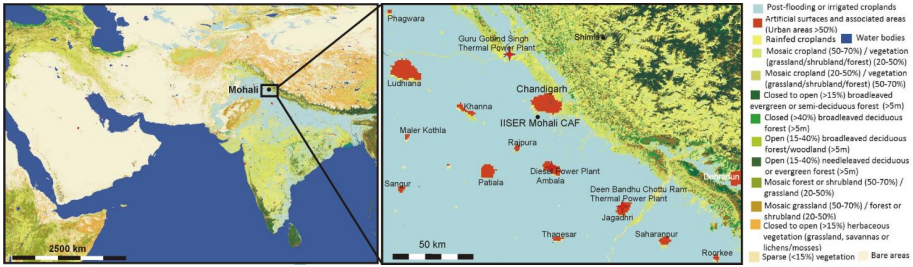

Figure 1. Left: location of Mohali on a land classification map (courtesy ESA GlobCover 2009 Project). The site is locatedin the north-west Indo-Gangetic plain, close to the forested slopes of the foothills of the Himalayan mountain range. Right: exact location of the measurement facility and its spatial relationship with respect to the nearby cities, the mountain range and potential local point sources of particulate matter.

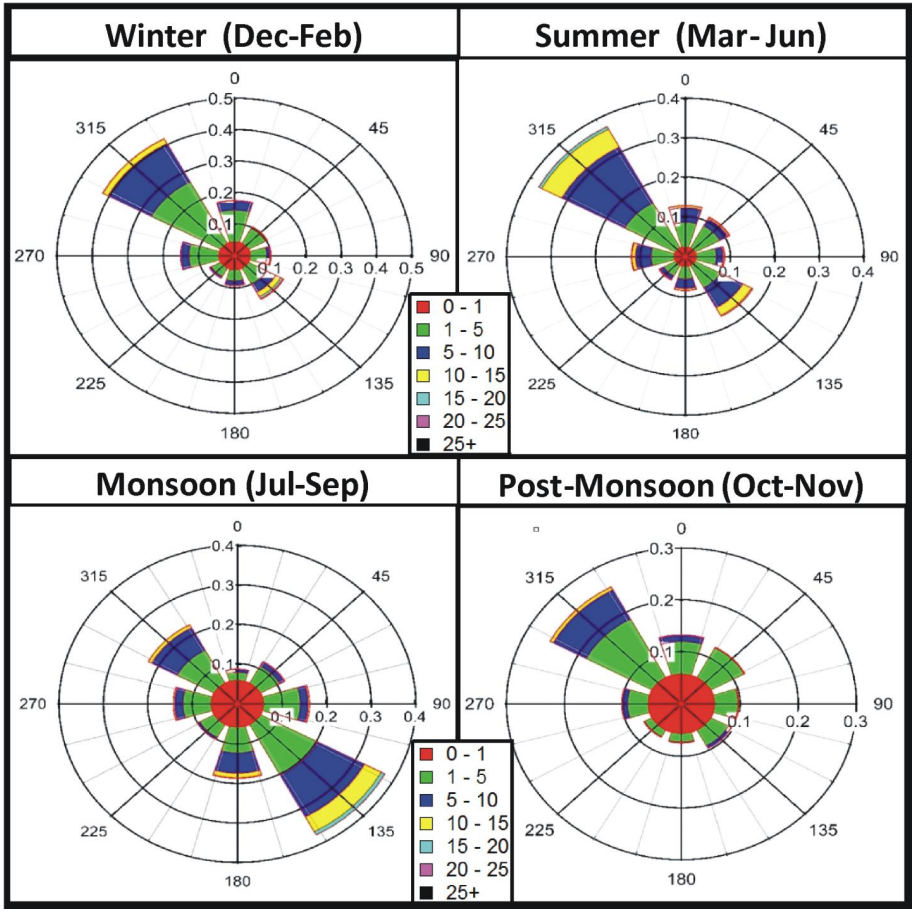

Figure 2. Wind rose plot for the measurement site for winter (December–February), summer (March–June), monsoon (July–September) and post-monsoon (October and November) season. BS: Wind speed and wind direction were measured at a height of 20 m a.g.l.

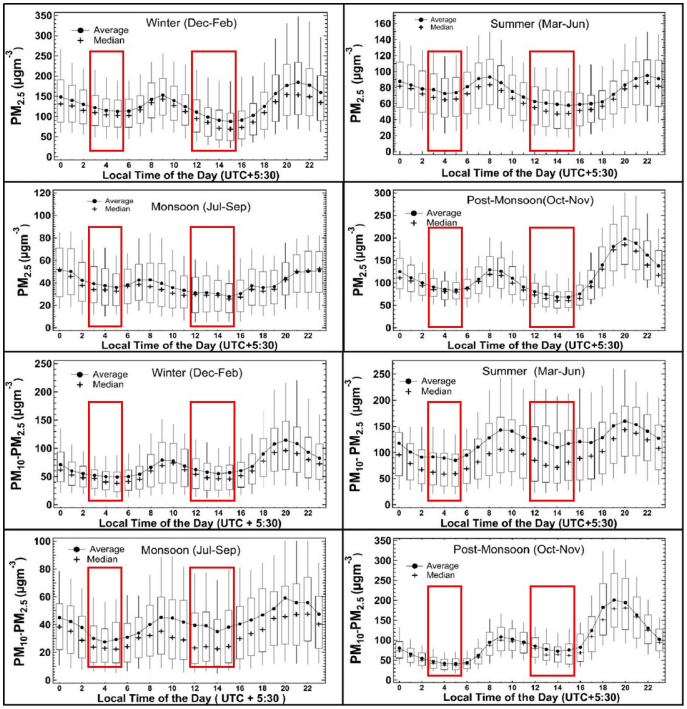

Figure 3. Diel box and whisker plots for fine mode (top four panels) and coarse mode (bottom four panels) particulate matter for winter, summer, monsoon and post monsoon season for the period November 2011 to August 2013 respectively. The box indicates the upper and lower quarter value; the cross indicates the median and the dots connected by lines provide the mean. The whiskers indicate the 5th and 95th percentile respectively. Periods of calm ($< 1\,\mathrm{m\,s^{-1}}$) have been excluded while preparing the graph. *BS:* The interval highlighted in red shows the daytime low (12 to 4 p.m. LT) and nighttime low (3 to 6 a.m. LT).

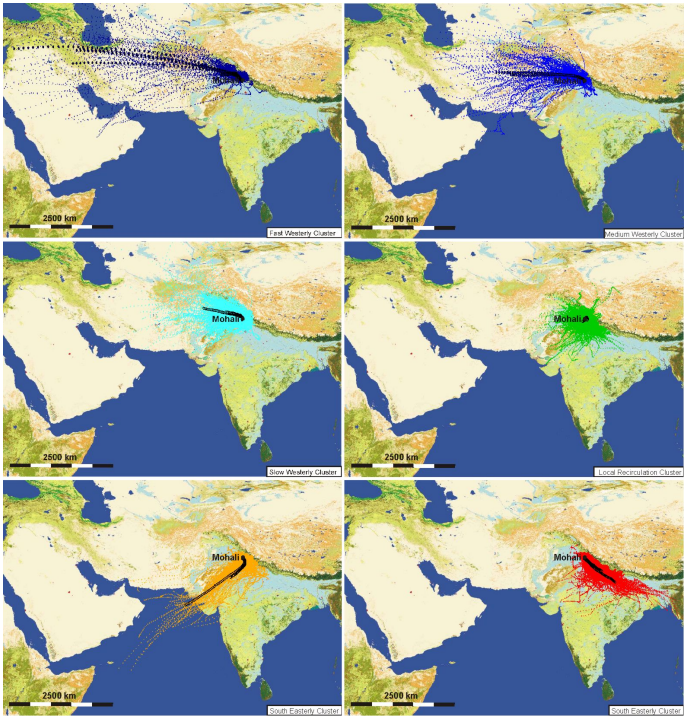

Figure 4. (**a–f**): All individual trajectories that contributed to each of the clusters [BS:]and the cluster average trajectories superimposed on a land classification map (courtesy ESA GlobCover 2009 Project). The length of each mean trajectory is 3 days and the distance between two successive data points represents a 1 h interval.The average trajectory of each cluster has been superiposed using circles with a black outline.

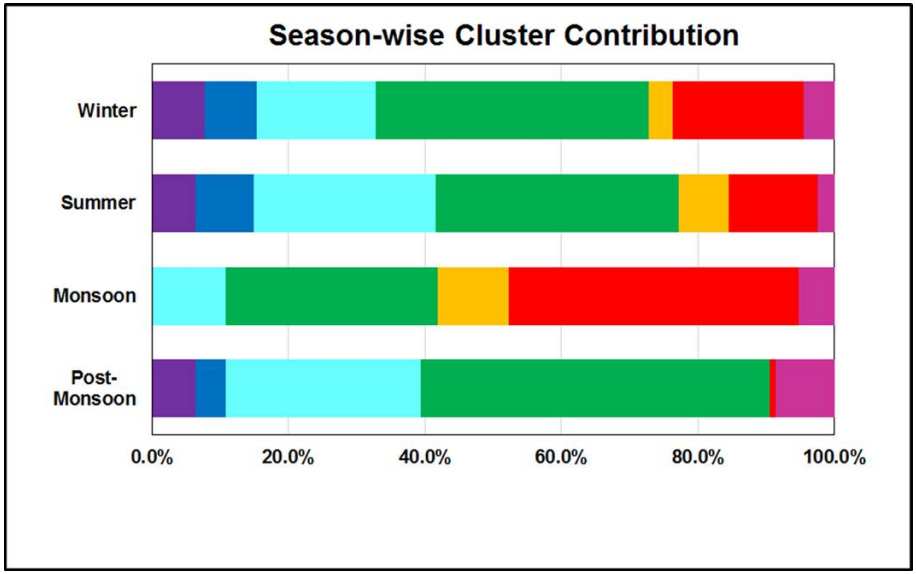

Figure 5. Contribution of individual clusters to air mass flow for all four seasons. Magenta: calm; red: south easterly cluster; orange: south westerly cluster; green: local cluster; light blue: slow westerly cluster; dark blue: medium westerly cluster; purple: fast westerly cluster.

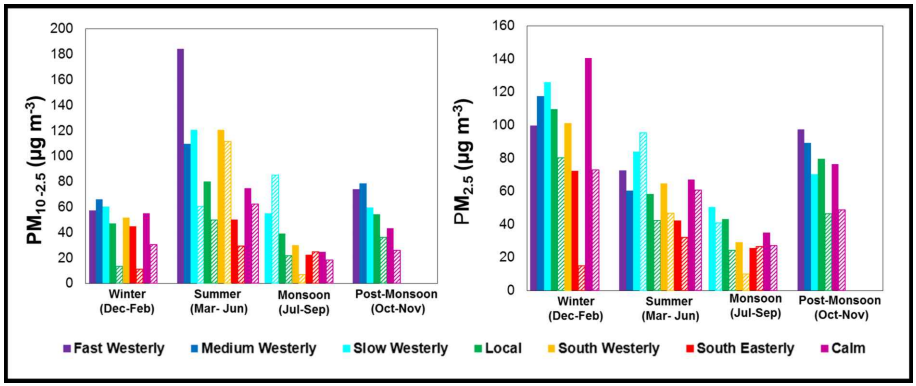

Figure 6. Mean coarse mode ($PM_{10-2.5}$) and fine mode ($PM_{2.5}$) mass loading for each air mass cluster and season at the IISER Mohali air quality station. Hatched bars indicate coarse mode and fine mode PM mass loadings observed during rain events.

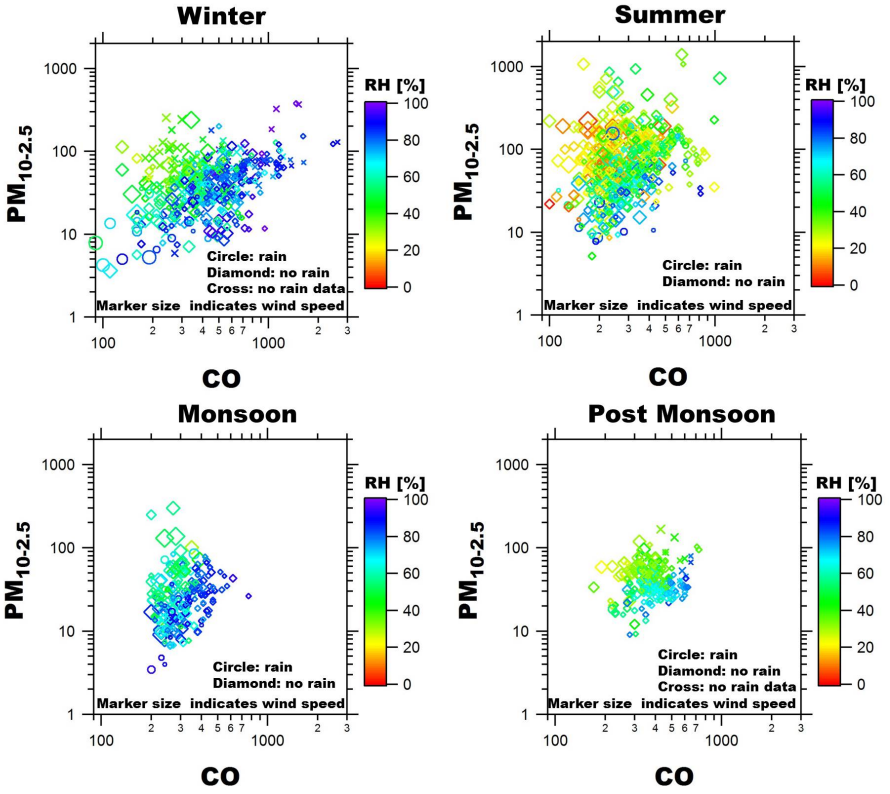

Figure 7. Dependence of coarse mode PM mass loadings on emission of gas phase precursors and meteorological parameters for the different seasons. The marker shape distinguishes PM mass loadings measured during rain events (circles) and under dry conditions (diamonds), data points obtained while the rain gauge was not working are marked with crosses. Marker size is proportional to wind speed. The smallest markers indicate WS $\leq 1\,\mathrm{m\,s^{-1}}$, the largest markers WS $\geq 15\,\mathrm{m\,s^{-1}}$. Markers are colour coded with relative humidity.

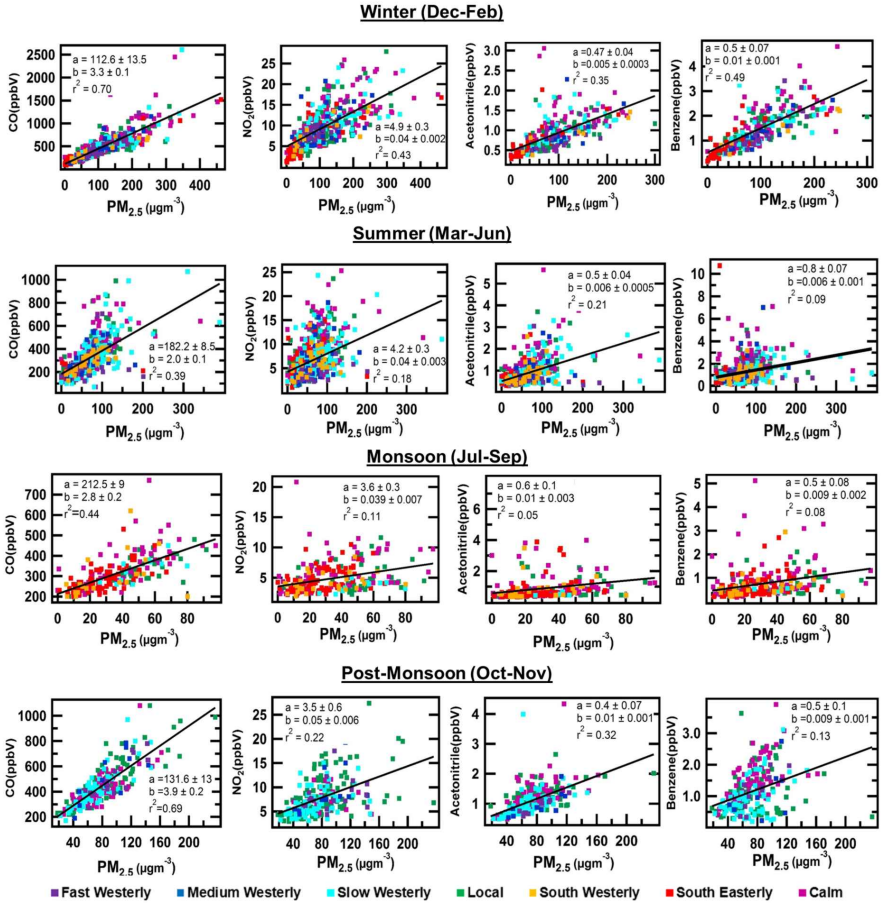

Figure 8. Scatter plots of fine mode PM with CO, acetonitrile, benzene and NO_2 for winter, summer, monsoon and post monsoon season. BS:"a" stands for intercept, "b" stands for slope in the linear regression equation.

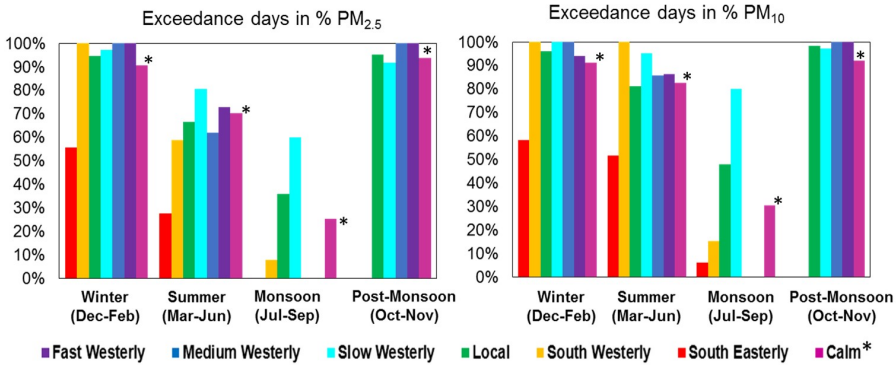

Figure 9. BS:Percentage of days where the 24 hour average PM_{10} BS: and $PM_{2.5}$ BS: mass loading (in $\mu g\,m^{-3}$ BS:)exceeds the national ambient air quality standard for each air mass cluster and season.*For calm conditions $PM_{2.5}$ BS: or PM_{10} BS: were averaged for all times during a 24 interval that had WS < 1 $m\,s^{-1}$ BS:only. The fraction of exceedance days is calculated based on this average, and not based on a genuine 24 hr average, as wind speeds do not remain low continuously.BS:~~Percentage of days where the median coarse mode (PM_{10} BS:) and fine mode ($PM_{2.5}$ BS:) mass loading (in $\mu g\,m^{-3}$ BS:) during the daytime/nighttime low exceeds the national ambient air quality standard for the 24 h BS: average for each air mass cluster and season.~~